

Research article

Courtney A. Puckree-Padua, Paul W. Gabrielson and Gavin W. Maneveldt*

DNA sequencing reveals three new species of *Chamberlainium* (Corallinales, Rhodophyta) from South Africa, all formerly passing under *Spongites yendoi*

<https://doi.org/10.1515/bot-2020-0074>

Received November 27, 2020; accepted December 18, 2020;
published online January 6, 2021

Abstract: Three new non-geniculate coralline algal species from South Africa are described that were passing under the misapplied name, *Spongites yendoi*. Based on plastid encoded DNA sequences from *psbA* and *rbcL* markers, these species belong in the subfamily Chamberlainoideae. The DNA sequences, supported by the morpho-anatomical character of tetrasporangial conceptacle roof development, placed all three species in the genus *Chamberlainium* and not *Pneophyllum*, the only other genus in Chamberlainoideae. In addition to the diagnostic DNA sequences, *Chamberlainium capense* sp. nov., *C. glebosum* sp. nov. and *Chamberlainium occidentale* sp. nov. may be distinguished by a combination of habit, habitat, geographic distribution, and several morpho-anatomical features. Biogeographically all three species are found in the Benguela Marine Province of South Africa, with *C. occidentale* being the most widespread. *Chamberlainium glebosum* also has a wide, but disjunct distribution and *C. capense* is another South African endemic non-geniculate coralline, whose range is restricted to a 43 km stretch of coastline. Thus far, DNA sequences from type specimens of non-geniculate corallines show that only those species whose type localities are from South Africa

are correctly applied; all other non-geniculate coralline names are likely misapplied in South Africa.

Keywords: biogeography; Chamberlainoideae; cryptic diversity; morpho-anatomy; non-geniculate coralline algae.

1 Introduction

The South African rocky intertidal and shallow subtidal zones have both an abundance and diversity of non-geniculate coralline red algae with three (Corallinales, Hapalidiales, Sporolithales; Stephenson and Stephenson 1972; Maneveldt et al. 2008) of the four orders (Corallinales, Corallinapetrales, Hapalidiales, Sporolithales; Jeong et al. 2020) represented. South Africa has representative species from more than half of the currently recognized extant genera of non-geniculate coralline red algae, with the order Corallinales best represented (Maneveldt et al. 2016). Included in this order are species previously placed in *Spongites* and the recently erected *Chamberlainium* that are particularly widespread and ecologically important in South Africa (Chamberlain 1993; Keats et al. 1993; Maneveldt and Keats 2008; Puckree-Padua et al. 2020b).

Based on a multi-gene molecular phylogeny, Rösler et al. (2016) noted that numerous southern hemisphere species, assigned to *Spongites*, did not occur in the same clade with the generitype, *Spongites fruticulosus* Kützinger (type locality: Mediterranean Sea), and would have to be placed in another genus. Caragnano et al. (2018) subsequently proposed a new genus *Chamberlainium* and a new subfamily Chamberlainoideae to accommodate sequenced and named *Spongites* species from the northeast Pacific and from South Africa (van der Merwe et al. 2015), making the new combinations *Chamberlainium tumidum* (Foslie) Caragnano, Foetisch, Maneveldt et Payri, *Chamberlainium decipiens* (Foslie) Caragnano, Foetisch, Maneveldt et Payri and *Chamberlainium agulhense* (Maneveldt, E. van der Merwe et P. W. Gabrielson) Caragnano, Foetisch, Maneveldt

*Corresponding author: Gavin W. Maneveldt, Department of Biodiversity and Conservation Biology, University of the Western Cape, P. Bag X17, Bellville 7535, South Africa, E-mail: gmaneveldt@uwc.ac.za. <https://orcid.org/0000-0002-5656-5348>

Courtney A. Puckree-Padua, Department of Biodiversity and Conservation Biology, University of the Western Cape, P. Bag X17, Bellville 7535, South Africa. <https://orcid.org/0000-0001-7684-0610>

Paul W. Gabrielson, Biology Department and Herbarium, University of North Carolina at Chapel Hill, Coker Hall CB 3280, Chapel Hill, NC, 27599-3280, USA. <https://orcid.org/0000-0001-9416-1187>

et Payri. Two morpho-anatomical characters were proposed to segregate *Chamberlainium* from *Spongites*: 1) diameter of tetra/bisporangial conceptacle chambers (<300 μm for *Chamberlainium* and >300 μm for *Spongites*); and 2) number of cell layers composing roofs of tetra/bisporangial conceptacles (≤ 8 cell layers for *Chamberlainium* and >8 for *Spongites*; Caragnano et al. 2018). The former of these characters no longer holds true for separating the genera morpho-anatomically (Puckree-Padua et al. 2020b).

Until recently, three species were recognized in *Spongites* in South Africa, based on morpho-anatomy, *Spongites impar* (Foslie) Y.M.Chamberlain (type locality: Cape Peninsula, Western Cape Province, South Africa), *Spongites discoideus* (Foslie) Penrose *et* Woelkerling (type locality mouth of the Rio Grande, Tierra del Fuego, Argentina), and *Spongites yendoi* (Foslie) Y.M.Chamberlain (type locality: Shimoda Harbor, Shimoda Prefecture, Japan). *Spongites impar* was transferred to *Chamberlainium* as *Chamberlainium impar* (Foslie) Puckree-Padua, P.W.Gabrielson *et* Maneveldt (Puckree-Padua et al. 2020b). The lectotype of *S. discoideus* was sequenced and shown to be distinct from South African specimens given that name and to belong in *Pneophyllum* to which it was transferred as *Pneophyllum discoideum* (Foslie) Puckree-Padua, Maneveldt *et* P.W.Gabrielson (Puckree-Padua et al. 2020a). An existing name was available for the South African *S. discoideus* specimens, *Lithophyllum marlothii* (Heydrich) Heydrich, whose type specimen was also sequenced, and it too was transferred to *Pneophyllum* as *Pneophyllum marlothii* (Heydrich) Puckree-Padua, P.W.Gabrielson, Hughey *et* Maneveldt (Puckree-Padua et al. 2020a).

In South Africa, based on morpho-anatomy, *S. yendoi* was considered to be variable in morphology (thin and featureless to thick and protuberant) and the most

ecologically important and abundant epilithic intertidal species along the entire South African coast of roughly 3000 km (Chamberlain 1993; Maneveldt and Keats 2008; Maneveldt et al. 2008). The species' morphological variability was largely attributed to variable grazing pressure and/or to sand scouring (Chamberlain 1993; Maneveldt and Keats 2008). Recently, DNA sequencing has resolved seven distinct species passing under *S. yendoi* in South Africa likely none of which are *S. yendoi* (Puckree-Padua et al. 2020b). Three of these species have already been treated, *Chamberlainium agulhense* (Caragnano et al. 2018; van der Merwe et al. 2015), *Chamberlainium cochleare* Puckree-Padua, Haywood, P.W.Gabrielson *et* Maneveldt, and *Chamberlainium natalense* (Foslie) Puckree-Padua, P.W.Gabrielson *et* Maneveldt (Puckree-Padua et al. 2020b). Herein we describe, name, and transfer to *Chamberlainium* three additional species. The seventh species, geographically distinct, which also was passing under *S. yendoi*, will be transferred later.

2 Materials and methods

Specimens were collected during spring low tides from the rocky intertidal and shallow subtidal at various locations along the South African coastline (Figure 1). Additional specimens from Namibia (southern West Africa), housed in the UWC herbarium, were also examined. Specimens on bedrock were removed using a geological hammer and chisel. Where specimens occurred on pebbles or gastropod shells, the entire pebble or shell along with the coralline was sampled. Specimens were sorted in the field. For each specimen, one fragment was air-dried, one placed in silica gel, and one fixed in 10% formalin.

Specimens for sequencing were examined and prepared following Gabrielson et al. (2011) and extracted following Hughey et al. (2001). Voucher specimens were deposited in UWC and NCU. Type

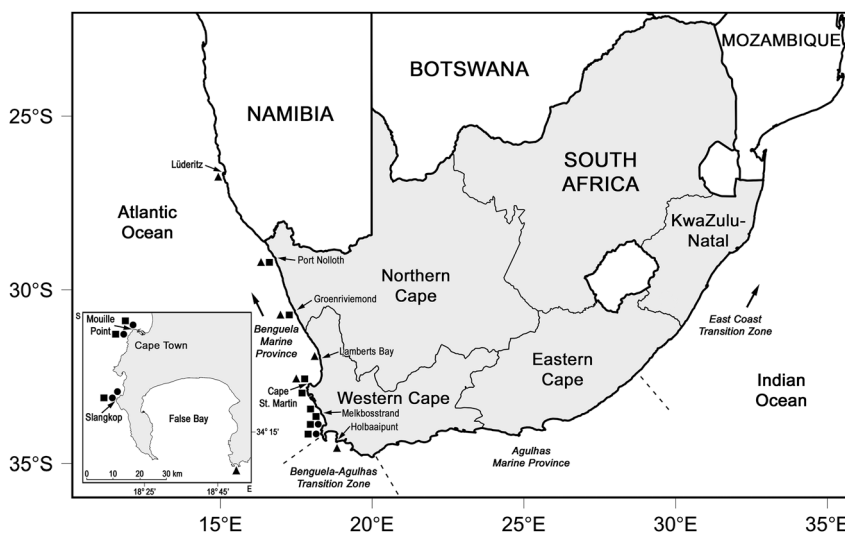


Figure 1: Map of South Africa (gray shade), with an inset of False Bay, showing the coastal provinces, the biogeographic marine provinces and the approximate locations of collecting sites (● = *Chamberlainium capense*, ■ = *C. glebosum*, ▲ = *C. occidentale*).

specimens were deposited in L (Naturalis, Netherlands, Leiden). Herbarium acronyms followed Thiers (2020, continuously updated).

Specimens for light microscopy were prepared following Maneveldt and van der Merwe (2012). In cell measurements, length denotes the distance between primary pit connections, and diameter the maximum width of the cell lumen at right angles to this. Conceptacle measurements followed Adey and Adey (1973). The determination and presentation (i.e., ranges and not averages with standard deviations/errors) of all measurements followed Maneveldt et al. (2017). Thallus anatomical terminology followed Chamberlain (1990). Growth form terminology, e.g., encrusting, warty, lumpy, followed Woelkerling et al. (1993).

Amplification of the *rbcl* marker was according to Gabrielson et al. (2011) and of the *psbA* marker according to Sissini et al. (2014). Resulting PCR products were sent to the DNA Analysis Core Facility at the University of North Carolina at Wilmington for sequencing and were manually aligned and compiled using Sequencher (Gene Codes Corp., Ann Arbor, Michigan, USA). Sequenced specimens are listed in Supplementary Table S1.

Used for the phylogenetic analyses were: 11 (of 31 – identical sequences removed) *psbA* sequences and 15 (of 24 – identical sequences removed) *rbcl* sequences from specimens previously assigned to *S. yendoii* from South Africa; six *psbA* and *rbcl* sequences from unknown species within Chamberlainoideae from Chile and Antarctica; one *psbA* sequence from a specimen assigned to *Pneophyllum fragile* Kützing from New Zealand; seven *psbA* and *rbcl* sequences from established species of *Chamberlainium*; three *psbA* and one *rbcl* sequence from established species of *Pneophyllum*; and an *S. fruticosus psbA* sequence (Supplementary Table S1). The *rbcl* and *psbA* sequences from the orders Gelidiales (one), Sporolithales (three), Hapalidiales (four and three respectively) and Corallinales (two) were used as outgroups in order to provide phylogenetic placement of Chamberlainoideae. Sequences from *P. fragile* specimens, from *Chamberlainium* specimens (van der Merwe et al. 2015) and outgroup sequences were obtained from GenBank. Outgroup sequence lengths ranged from 293 to 1364 bp. The remaining *psbA* and *rbcl* sequences ranged between 629–851 bp and 691–1387 bp long, respectively. Sequences for each gene were aligned using MUSCLE (Edgar 2004), as implemented in Geneious, with a maximum of eight iterations.

Geneious v11.1.5 (<https://www.geneious.com>, Kearse et al. 2012) was used for all phylogenetic analyses. Identical sequences were removed from the respective datasets before Maximum Likelihood (RAxML, Stamatakis 2006) analyses were performed on 38 *psbA* and 39 *rbcl* sequences separately using the GTR CAT model of evolution applying the Rapid-hill climbing algorithm with 10 topological searches from random starts and then Rapid Bootstrapping and search for best-scoring ML tree algorithm, with 500 bootstrap replicates.

Bayesian analyses were performed on 38 unique *psbA* and 39 unique *rbcl* sequences using the Geneious v11.1.5 (<https://www.geneious.com>, Kearse et al. 2012) MrBayes v3.2.6 plugin (Huelsenbeck and Ronquist 2001). Under the GTR model, sampling was performed every 1000 generations. Analyses were run for 1.1 million generations with a 100 000 burn-in.

3 Results

A total of 58 *psbA* sequences (31 newly generated and 27 from GenBank) and 48 *rbcl* sequences (24 newly generated

and 24 from GenBank) were used in the phylogenetic analyses (Supplementary Table S1). The RAxML and Bayesian analyses, for both the *psbA* (Figure 2) and *rbcl* (Figure 3) genes were congruent in resolving *Chamberlainium capense* sp. nov., *Chamberlainium glebosum* sp. nov. and *Chamberlainium occidentale* sp. nov. in a monophyletic clade in Chamberlainoideae with full support (100% BS/1 PP). These three species occurred in a clade with the generitype of *Chamberlainium*, *C. tumidum*, in both *psbA* (82/0.97, Figure 2) and *rbcl* (99/1, Figure 3) trees. In the *psbA* tree, *C. glebosum* and *Chamberlainium capsense* are sister species with moderate support (76/0.93) with *C. occidentale* sister to that pair with full support, whereas in the *rbcl* tree, *C. occidentale* and *C. capsense* are sister species with strong support (96/1) with *C. glebosum* sister to that pair again with full support. Both genes show support

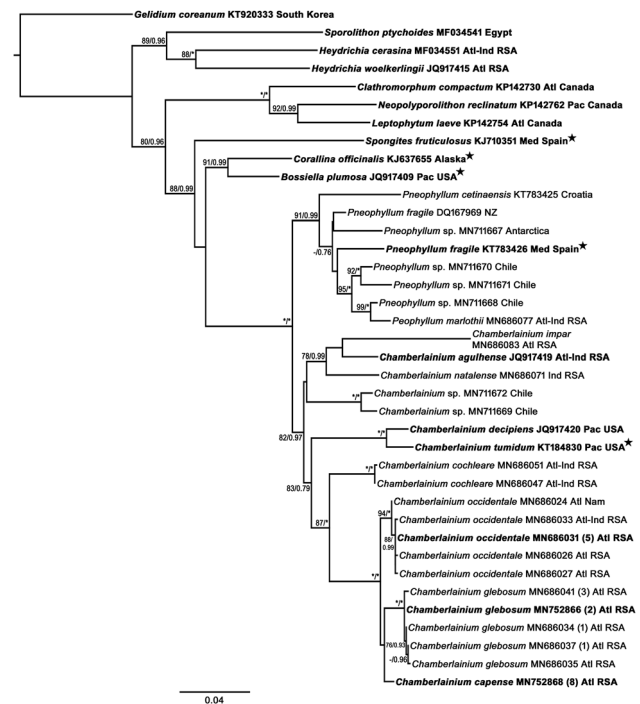


Figure 2: Maximum likelihood tree based on *psbA* sequences. Species with sequenced type/'topotype' material are highlighted in bold. Generitype species and molecular references for generitype species within the Corallinales are identified by a star (★). Species names are followed by their GenBank accession number and their geographic location, including ocean basin where needed. Numbers in brackets, following the GenBank accession numbers, are the total number of identical sequences. Bootstrap support (BS) and Bayesian posterior probability (BPP) values are provided at branch nodes. BS and BPP values = 100% and = 1 respectively, are denoted by an asterisk (*); BS and BPP values <75 % and < 0.75 respectively, are not shown. Atl = Atlantic Ocean, Ind = Indian Ocean, Med = Mediterranean, Nam = Namibia, NZ = New Zealand, Pac = Pacific Ocean.

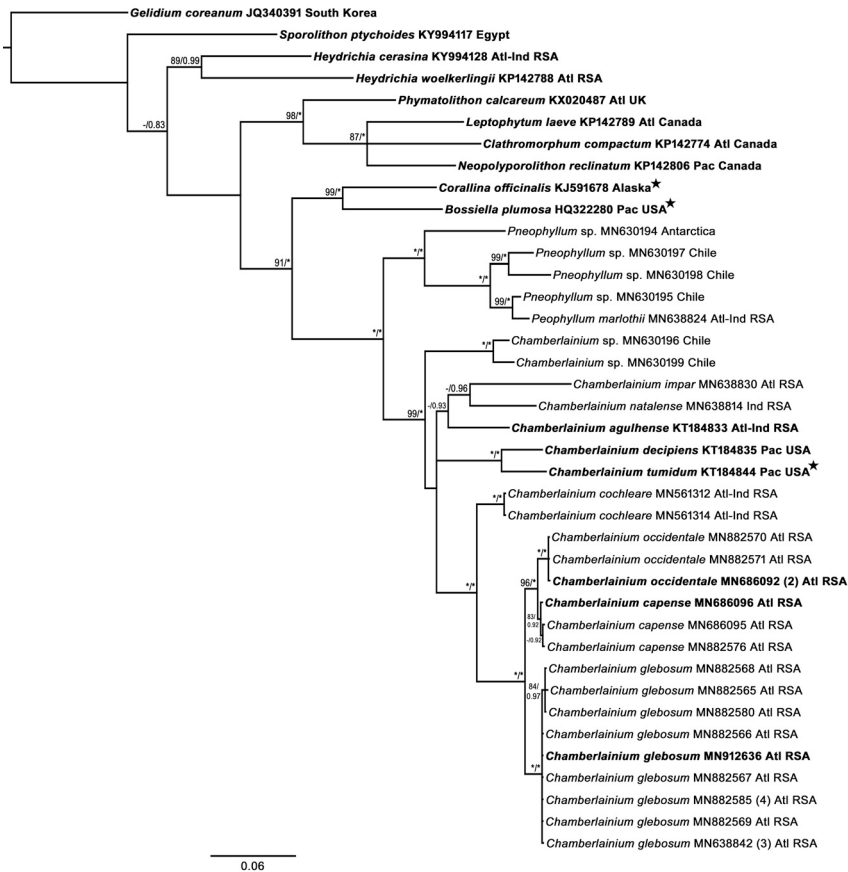


Figure 3: Bayesian inference tree based on *rbcL* sequences. Species with sequenced type/topotype material are highlighted in bold. Generitype species within Corallinales are identified by a star (★). Species names are followed by their GenBank accession number and their geographic location, including ocean basin where needed. Numbers in brackets, following the GenBank accession numbers, are the total number of identical sequences. Bootstrap support (BS) and Bayesian posterior probability (BPP) values are provided at branch nodes. BS and BPP values = 100 % and = 1 respectively, are denoted by an asterisk (*); BS and BPP values < 75 % and < 0.75 respectively. Atl = Atlantic Ocean, Ind = Indian Ocean, Med = Mediterranean, Pac = Pacific Ocean.

for *C. cochleare* sister to the *C. capense* + *C. glebosum* + *C. occidentale* clade, moderate for *psbA* (83/0.79), full for *rbcL* (100/1). In the *psbA* tree (Figure 2), the clade formed by *C. cochleare*, *C. capense*, *C. glebosum* and *C. occidentale* is weakly supported (83/0.79) as sister to two northeast Pacific species, *C. tumidum* and *C. decipiens*; in the *rbcL* tree (Figure 3) the relationship of these northeast Pacific species is unresolved with respect to the other *Chamberlainium* species.

Interspecific sequence divergences for the *psbA* gene ranged from 1.71 to 11.59% for *Chamberlainium* species, whereas intraspecific sequence divergences ranged from 0 to 1.41% (Supplementary Table S2). For *psbA*, *C. capense* differed from *C. glebosum* by 3.14%, from *C. occidentale* by 2.84%, and *C. glebosum* from *C. occidentale* by 3.51%. Interspecific sequence divergences for the *rbcL* gene ranged from 0.98 to 12.19% for *Chamberlainium* species, whereas intraspecific sequence divergences ranged from 0 to 0.17% (Supplementary Table S3). For *rbcL*, *C. capense* differed from *C. glebosum* by 2.25%, from *C. occidentale* by 0.98%, and *C. glebosum* from *C. occidentale* by 2.68%.

For all taxa, morpho-anatomy was done only on sequenced specimens. See Supplementary Table S4 for collection details.

***Chamberlainium capense* Puckree-Padua, P.W. Gabrielson et Maneveldt sp. nov.** (Figures 4, 7–11, 12–14, 15–18; Tables 1, 2).

Holotype: L 3986119, 09.x.2016, *leg. G.W. Maneveldt*, collection number 16/05, epilithic on primary bedrock in mid-intertidal, sand inundated rock pool.

Type locality: South Africa, Western Cape Province, Mouille Point (33°53.9440' S, 18°24.5285' E).

Etymology: ‘*capense*’ in reference to the species’ restricted distribution along the Cape Peninsula historically known as the ‘Cape of Good Hope, South Africa’ (*Caput Bonae Spei*).

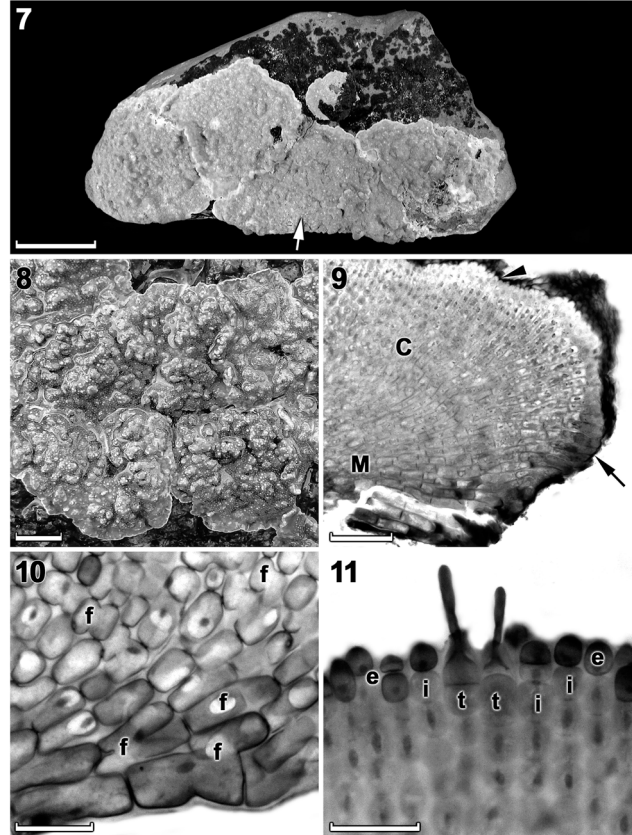
Description: Non-geniculate, thalli are moderately thick (up to 1000 μm), encrusting to mostly variably lumpy to slightly protuberant. Thalli are epilithic or epizoid and bright to dusky pink in well-lit conditions. Individual crusts do not appear to fuse together and are easily discernible. Thallus construction is monomerous with a single layer of epithallial cells. A central columella is present in tetrasporangial conceptacles that disintegrate to form a low mound with maturity. The pore opening in mature tetrasporangial conceptacles is occluded by a corona of filaments that projects above the opening. The *psbA* (851 bp) and *rbcL* (691–1387 bp) sequences are diagnostic.



Figures 4–6: Habit photographs of *Chamberlainium capense*, *C. glebosum* and *C. occidentale*. (4) *Chamberlainium capense* is moderately thick to mostly lumpy and only slightly protuberant. Scale bar = 20 mm. (5) *Chamberlainium glebosum* is thick, very lumpy and highly protuberant. Scale bar = 20 mm. (6) *Chamberlainium occidentale* is morphologically highly variable, occurring as thin encrusting (smooth) to thick warty (mostly) to lumpy plants, and are only slightly protuberant. Scale bar = 30 mm.

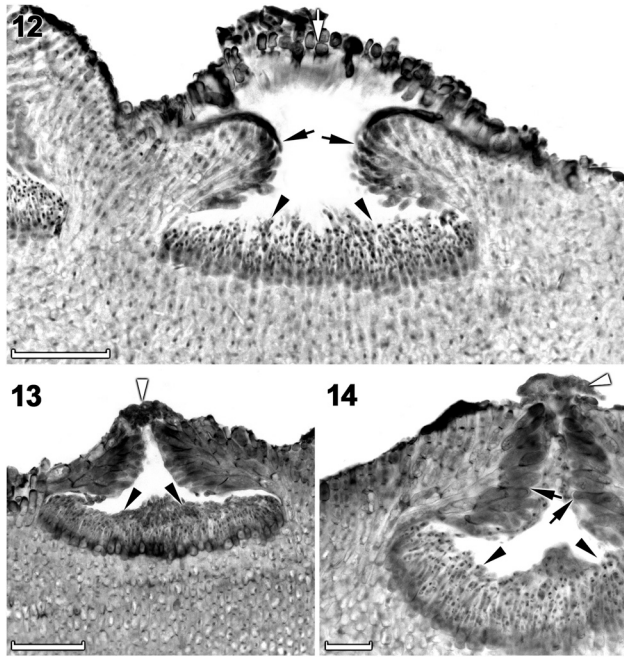
Habitat: Thalli were epilithic on the primary bedrock and on large boulders in rock pools and on exposed platforms in the mid-intertidal zone, as well as epizoic on mollusc shells in the low intertidal zone.

Vegetative morphology and anatomy: Thalli were non-geniculate, moderately thick (up to 1000 μm), encrusting (smooth) to mostly variably lumpy and slightly protuberant, with protuberances to 4 mm tall (Figures 4 and 7, 8), and were firmly adherent, dusky pink to mauve (in well-lit conditions) to rosy or purple-pink (in dim light) when freshly collected (Figure 4). Individual crusts did not fuse together and were easily discernible (Figures 7, 8).



Figures 7–11: *Chamberlainium capense* habit and vegetative anatomy. (7) Rock fragment showing holotype specimen (white arrow) (L 3986119, tetrasporangial). Scale bar = 20 mm. (8) Encrusting to variably lumpy and slightly protuberant, epilithic thalli showing crusts abutting and easily discernible. Scale bar = 10 mm. (9) Vertical section through the margin (black arrow) showing the monomerous thallus construction with plumose medulla (M) giving rise to cortical filaments (C) that terminate in a single layer of epithallial cells (black arrowhead) (UWC 16/17). Scale bar = 50 μm . (10) Vertical section of the inner thallus showing cell fusions (f) between adjacent medullary filaments (UWC 16/17). Scale bar = 20 μm . (11) Vertical section of the outer thallus showing a single layer of epithallial cells (e) subtended by a layer of subepithallial initials (i). Note the paired, bottle-shaped trichocytes (t) (UWC 16/24). Scale bar = 20 μm .

Thalli were dorsiventrally organized, monomerous and haustoria were absent. The medulla was thin and plumose (non-coaxial) (Figures 9, 10). Medullary filaments comprised rectangular to elongate cells, which gave rise to cortical filaments that comprised mainly square to rectangular cells (Figure 10). Contiguous medullary and cortical filaments were joined by cell fusions; secondary pit connections were absent (Figure 10). Subepithallial initials (intercalary meristematic cells) were square to rectangular (Figure 11). The epithallus was single layered with oval to rounded cells (Figure 11). Trichocytes were common at the



Figures 12–14: *Chamberlainium capense* spermatangial anatomy (UWC 16/21). (12) Vertical section through the outer thallus showing a spermatangial conceptacle primordium with peripheral roof development (black arrows) and simple, spermatangial systems (black arrowheads) confined to the conceptacle floor. Note the protective layer of epithallial cells (white arrow). Scale bar = 50 μm . (13) Vertical section through a mature, raised spermatangial conceptacle showing the mucilage plug (white arrowhead) that occludes the pore opening and simple, spermatangial systems (black arrowheads) confined to the conceptacle floor. Scale bar = 50 μm . (14) Magnified view through a mature spermatangial conceptacle showing the mucilage plug (white arrowhead) that occludes the pore opening and simple, spermatangial systems (black arrowheads) confined to the conceptacle floor. Note that the pore canal is lined with terminal, elongate initials (black arrows) that project into the pore canal as papillae. Scale bar = 20 μm .

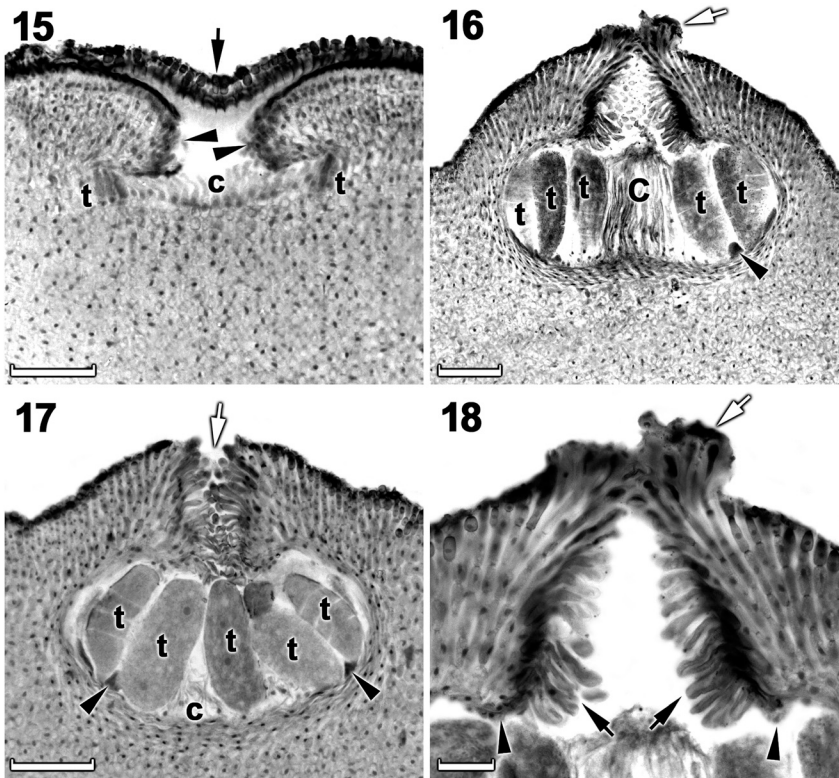
thallus surface and occurred singularly (mostly) to paired (Figure 11). Trichocytes were always terminal and never intercalary in the cortex; buried trichocytes were not observed. Data on morphological and measured vegetative characters are summarized in Table 1.

Reproductive morphology and anatomy: Gametangial thalli appeared to be dioecious, although female plants were not observed.

Spermatangial (male) conceptacles were uniporate, low-domed and raised above surrounding thallus surface (Figures 12–14). Conceptacle chambers were transversely elliptical to flatten; conceptacle roof nearly twice as thick along pore canal (Figures 13, 14). Conceptacle roof formed from filaments peripheral to the fertile area (Figure 12). Throughout the early development, a protective layer of epithallial cells surrounded the conceptacle primordium

(Figure 12). This protective layer was shed once the pore canal was near fully developed. The pore opening was occluded by a mucilage plug (Figures 13, 14). In mature conceptacles, terminal initials along pore canal were enlarged and papillate; they projected into the pore canal and were orientated more or less parallel to the conceptacle roof surface (Figure 14). Unbranched (simple) spermatangial systems were confined to mature conceptacle floor (Figures 12–14). Senescent male conceptacles appeared to be shed; no buried conceptacles were observed.

Tetrasporangial thalli were morphologically similar to spermatangial thalli. Conceptacles were uniporate, low domed and raised above the surrounding thallus surface (Figures 15–17). Conceptacle chambers were transversely elliptical to bean-shaped. Conceptacle roof was nearly twice as thick along the pore canal and was 5–7 cells thick, including an epithallial cell. Pore canal tapered towards the surface, formed an arch (Figure 18) and was lined by elongated papillate cells that projected into the canal and were orientated more or less parallel or nearly perpendicular to the conceptacle roof surface (Figure 18). The roof was formed from filaments peripheral to the fertile area (Figure 15) and terminal initials were more elongate than their inward derivatives. Throughout early development a protective layer of epithallial cells surrounded the conceptacle primordium (Figure 15). This protective layer was shed once pore canal was near fully developed; the pore opening was occluded by a corona of filaments that projected above the pore opening (Figures 16, 18). The corona appeared to form from filaments near the upper half of the roof, directly adjacent to the pore canal (Figures 16, 18). Throughout the development of the tetrasporangial conceptacle, a prominent columella of sterile filaments formed at the center of the conceptacle chamber (Figure 15), which extended into the pore canal (Figure 16); the central columella appeared weakly calcified as with maturity it disintegrated to form a low mound (Figure 17). The base of the pore canal was sunken into the chamber and terminal initials near the base pointed downward (Figure 18). Mature conceptacle floors were sunken 11–17 cells (including the epithallial cell) below the surrounding thallus surface. Zonately divided tetrasporangia were arranged at the extreme periphery of the conceptacle chamber and were attached via a stalk cell (Figures 16, 17). Where the central columella had disintegrated or diminished, the tetrasporangia filled the chamber and appeared to be distributed across the chamber floor (Figure 17). Senescent tetrasporangial conceptacles appear to be shed as no buried conceptacles were observed. Data on reproductive characters are summarized in Table 2.



Figures 15–18: *Chamberlainium capense* tetrasporangial anatomy. (15) Vertical section through the outer thallus showing a later stage tetrasporangial conceptacle primordium with peripheral roof development (black arrowheads) and tetrasporangial initials (t) arranged peripherally around a central columella (c). Note the persisting layer of protective epithallial cells (black arrow) (L 3986119). Scale bar = 50 μm . (16) Vertical section through a mature, raised tetrasporangial conceptacle showing tetrasporangia (t) with a stalk cell (black arrowhead), peripherally arranged around a well-defined central columella (C). Note the remains of a corona (white arrow) that surrounds the pore opening (L 3986119). Scale bar = 50 μm . (17) Vertical section through a mature raised tetrasporangial conceptacle showing tetrasporangia (t) with stalk cells (black arrowheads), appearing to be arranged across the chamber floor as the columella (c) has disintegrated. Note the absence of the corona (white arrow) (UWC 16/09). Scale bar = 50 μm . (18) Magnified view of the pore canal of a mature tetrasporangial conceptacle showing the base of the pore canal sunken (black arrowheads) into the chamber with terminal, elongate initials near the base pointing downward (black arrows) and the remains of a corona (white arrow) that surrounds and occludes the pore opening. (L 3986119). Scale bar = 20 μm .

Distribution: Confirmed by DNA sequences to have a restricted distribution (± 43 km distance) along the southwest coast, from Mouille Point to Slangkop (Western Cape Province) along the Cape Peninsula, South Africa.

***Chamberlainium glebosum* Puckree-Padua, P.W. Gabrielson et Maneveldt sp. nov.** (Figures 5, 19–23, 24–25, 26–30; Tables 1, 2).

Holotype: L 3986123, 17vii.2015, leg. G.W. Maneveldt, collection number 18/05, epilithic on primary bedrock in a mid-intertidal rock pool.

Type locality: South Africa, Western Cape Province, Melkbosstrand (33°44.2518' S, 18°26.1343' E).

Etymology: ‘*glebosum*’ from ‘*glebosus*’, making reference to the species’ lumpy (Stearn 1973) and highly protuberant growth form.

Description: Non-geniculate, thalli are thick (to 2000 μm), very lumpy becoming highly protuberant. Thalli are epilithic and brownish pink to gray in well-lit conditions. Individual crusts do not appear to coalesce (do not fuse together) and are easily discernible. The thallus construction is monomerous with a single layer of epithallial cells. A central columella is present in tetrasporangial conceptacles, which disintegrates to form a low mound with maturity. The pore opening in mature tetrasporangial conceptacles is unoccluded. The *psbA* (851 bp) and *rbcL* (691–1387 bp) gene sequences are diagnostic.

Habitat: Thalli were epilithic on the primary bedrock in the high and mid-intertidal zones and only occasionally on the low shore.

Vegetative morphology and anatomy: Thalli were non-geniculate, thick (up to 2000 μm), very lumpy

Table 1: Comparison of the appearance and vegetative structure of South African species formally ascribed to *Chamberlainium*.

| Character | <i>Chamberlainium agulhense</i> (van der Merwe et al. 2015) | <i>Chamberlainium capemse</i> (this study) | <i>Chamberlainium cochleare</i> (Puckree-Padua et al. 2020b) | <i>Chamberlainium glebosum</i> (this study) | <i>Chamberlainium impar</i> (Puckree-Padua et al. 2020b) | <i>Chamberlainium natalense</i> (Puckree-Padua et al. 2020b) | <i>Chamberlainium occidentale</i> (this study) |
|--------------------------------|---|--|--|---|--|--|--|
| Growth form | Encrusting (smooth) | Encrusting (smooth), becoming variably lumpy (mostly) and slightly protuberant | Encrusting (smooth) | Lumpy, becoming highly protuberant | Encrusting (smooth), orbicular becoming confluent | Encrusting (smooth) | Encrusting (smooth) to warty (mostly) to lumpy, becoming slightly protuberant |
| Thallus construction | Dimerous | Monomeric | Monomeric | Monomeric | Monomeric | Monomeric | Monomeric |
| Maximum thallus thickness | 650 | 1000 | 370 | 2000 | 1800 | 800 | 1000 |
| Habit | Individual thalli discernible, not fusing | Individual thalli discernible, not fusing | Individual thalli not discernible, fusing to form large expanses | Individual thalli discernible, not fusing | Individual thalli discernible, not fusing | Individual thalli discernible, not fusing | Individual thalli discernible, not fusing |
| Trichocytes | None observed | Common, solitary (mostly) to paired | Common, solitary (mostly) to clustered, up to 6 (separated by normal vegetative filaments) | None observed | Rare, solitary to paired | Rare, solitary (mostly) to clustered, up to 6 (separated by normal vegetative filaments) | Common, solitary (mostly) to clustered, up to 6 (separated by normal vegetative filaments) |
| Trichocyte dimensions | - | $L = 22-29; D = 5-7$ | $L = 15-27; D = 7-12$ | - | $L = 22-39; D = 10-12$ | $L = 12-29; D = 7-10$ | $L = 22-37; D = 7-10$ |
| No. of epithallial cell layers | 1-3 (mostly 1-2) | 1 | 1 | 1 | 4-6 (9) | 1 | 1 |
| Epithallial cell shape | Rounded to domed | Oval to round | Elliptical to domed | Rounded to elliptical | Elliptical to rounded | Flattened to elliptical | Elliptical to rounded to elongate |
| Epithallial cell dimensions | ND | $L = 5-7; D = 5-7$ | $L = 2-7; D = 5-7$ | $L = 5-7; D = 2-7$ | $L = 5-7; D = 5-7$ | $L = 5-7; D = 5-7$ | $L = 5-8; D = 2-7$ |
| Subepithallial cell shape | Square to rectangular | Square to rectangular | Square to rectangular | Rectangular | Square to rectangular | Square to rectangular | Rectangular |
| Subepithallial cell dimensions | ND | $L = 5-15; D = 5-10$ | $L = 3-10; D = 4-7$ | $L = 5-12; D = 2-7$ | $L = 5-12; D = 5-7$ | $L = 7-10; D = 5-7$ | $L = 10-12; D = 5-7$ |
| Cortical cell shape | - | Square to rectangular | Square to rectangular | Square to rectangular | Square to beaded | Square to rectangular | Square to rectangular |
| Cortical cell dimensions | - | $L = 7-10; D = 7-10$ | $L = 5-12; D = 4-12$ | $L = 5-15; D = 5-0$ | $L = 7-10; D = 2-5$ | $L = 7-25; D = 5-7$ | $L = 7-10; D = 7-12$ |
| Medullary cell shape | - | Rectangular | Rectangular to elongate | Rectangular to elongate | Rectangular to elongate | Rectangular to elongate | Square to rectangular |
| Medullary cell dimensions | - | $L = 22-44; D = 15-25$ | $L = 10-30; D = 3-16$ | $L = 12-25; D = 7-12$ | $L = 5-25; D = 7-14$ | $L = 15-20; D = 5-7$ | $L = 15-17; D = 7-10$ |
| Erect filament cell shape | Square to rectangular with rounded corners | - | - | - | - | - | - |

Table 1: (continued)

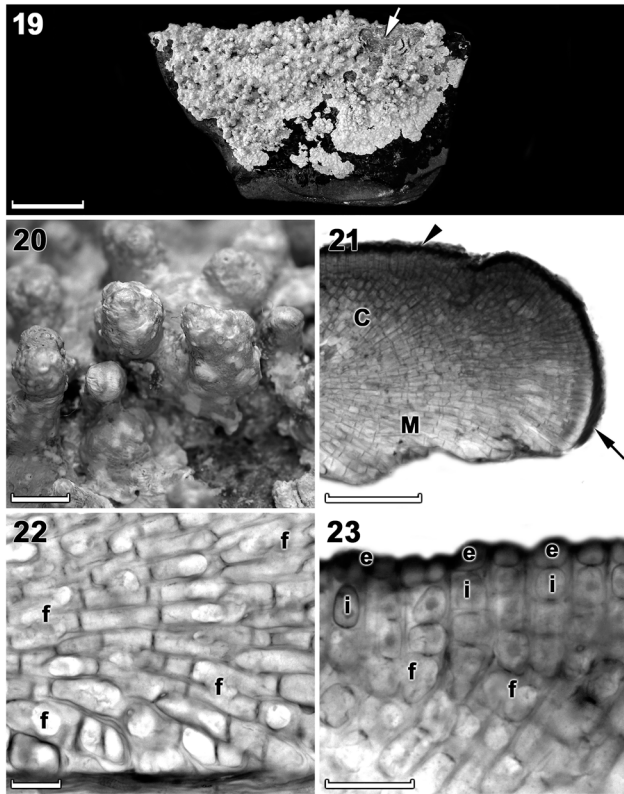
| Character | <i>Chamberlainium agulhense</i> (van der Merwe et al. 2015) | <i>Chamberlainium capemse</i> (this study) | <i>Chamberlainium cochleare</i> (Puckree-Padua et al. 2020b) | <i>Chamberlainium glebosum</i> (this study) | <i>Chamberlainium impar</i> (Puckree-Padua et al. 2020b) | <i>Chamberlainium natalense</i> (Puckree-Padua et al. 2020b) | <i>Chamberlainium occidentale</i> (this study) |
|---|---|--|--|---|--|--|--|
| Erect filament cell dimensions | ND | - | - | - | - | - | - |
| Basal filament cell shape (in radial view) | Non-palisade, irregularly square | - | - | - | - | - | - |
| Basal filament cell dimensions (in radial view) | $L = 10-29; H = 10-22$ | - | - | - | - | - | - |
| Basal filament cell shape (in tangential view) | Rectangular to palisade-like | - | - | - | - | - | - |
| Basal filament cell dimensions (in tangential view) | $L = 10-22; H = 5-10$ | - | - | - | - | - | - |

Unless otherwise stated, all measurements are in micrometers. L , H and D , length, height and diameter, respectively; ND, no data provided.

Table 2: Comparison of the reproductive structures of South African species formally ascribed to *Chamberlainium*.

| Character | <i>Chamberlainium agulhense</i> (van der Merwe et al. 2015) | <i>Chamberlainium capense</i> (this study) | <i>Chamberlainium cochleare</i> (Puckree-Padua et al. 2020b) | <i>Chamberlainium glebosum</i> (this study) | <i>Chamberlainium impar</i> (Puckree-Padua et al. 2020b) | <i>Chamberlainium natalense</i> (Puckree-Padua et al. 2020b) | <i>Chamberlainium occidentale</i> (this study) |
|--|---|--|---|--|--|---|--|
| Mature tetrasporangial pore characteristics | Pore opening occluded and flush with surrounding roof | Pore opening occluded by a corona of filaments and flush with surrounding roof | Pore opening occluded by a mucilage plug and flush with surrounding roof | Pore opening occluded and flush with surrounding roof | Pore opening occluded by a mucilage plug and flush with surrounding roof | Pore opening occluded by a corona of filaments and flush with surrounding roof | Pore opening occluded and slightly sunken below the surrounding roof |
| Thickness of mature tetrasporangial conceptacle roof | 29–47 | 47–96 | 29–76 | 27–115 | 47–61 | 27–66 | 42–83 |
| No. of cells (incl. epithalial cells) in mature tetrasporangial conceptacle roof | 4–8 | 5–7 | 6–8 | 4–9 | 6–7 | 6–8 | 5–7 |
| Depth (no. of cells) of mature tetrasporangial conceptacle floor | 10–15 | 11–17 | 12–22 | 11–24 | 15–21 | 12–21 | 16–19 |
| Shape of pore canal | Pore canal not arching, tapered towards surface | Pore canal arching, tapered towards surface | Pore canal not arching, tapered towards the surface or straight in senescing conceptacles | Pore canal not arching, tapered towards surface | Pore canal not arching, tapered towards surface | Pore canal not arching, tapered towards the surface or straight in very mature conceptacles | Pore canal arching, tapered towards surface |
| Tetrasporangia dimensions | ND | $L = 51–130; D = 22–44$ | $L = 47–79; D = 20–40$ | $L = 29–113; D = 5–69$ | $L = 54–98; D = 29–44$ | $L = 44–81; D = 20–49$ | $L = 74–152; D = 42–61$ |
| Tetrasporangia arrangement | Peripheral | Peripheral, may appear distributed across chamber floor as columella disintegrates | Peripheral | Peripheral | Peripheral | Peripheral, may appear distributed across chamber floor as columella disintegrates | Peripheral, may appear distributed across chamber floor as columella disintegrates |
| Central columella | Prominent; disintegrates to form a low mound with maturity | Prominent; disintegrates to form a low mound with maturity | Prominent; disintegrates to form a low mound with maturity | Prominent; disintegrates to form a low mound with maturity | Prominent; persists to maturity | Prominent; disintegrates to form a low mound with maturity | Prominent; disintegrates to form a low mound with maturity |
| Conceptacles buried or shed | Shed | Shed | Shed | Shed | Shed | Conceptacles mostly shed; occasionally tetrasporangia and spermatangia may be found buried | Shed |

Unless otherwise stated, all measurements are in micrometers. *L* and *D*, length and diameter respectively; ND, no data provided.



Figures 19–23: *Chamberlainium glebosum* habit and vegetative anatomy. (19) Rock fragment with holotype specimen showing the region (white arrow) of the holotype from which all analyses were done (L 3986123, tetrasporangial). Scale bar = 20 mm. (20) Magnified view showing highly protuberant nature of *C. glebosum* holotype specimen (L 3986123). Scale bar = 2 mm. (21) Vertical section through the margin (black arrow) showing the monomerous thallus construction with plumose medulla (M) giving rise to cortical filaments (C) that terminate in a single layer of epithallial cells (black arrowhead) (UWC 15/34). Scale bar = 100 µm. (22) Vertical section of the inner thallus showing cell fusions (f) between adjacent medullary filaments (UWC 15/34). Scale bar = 10 µm. (23) Vertical section of the outer thallus showing a single layer of epithallial cells (e) subtended by a layer of subepithallial initials (i). Note the cell fusions (f) between adjacent cortical filaments (UWC 15/34). Scale bar = 20 µm.

becoming highly protuberant with protuberances to 6 mm tall (Figures 5, 19 and 20), and were firmly adherent, mostly brownish pink to greyish when freshly collected (Figure 5). Individual crusts did not coalesce (did not fuse together) and were easily discernible (Figure 5).

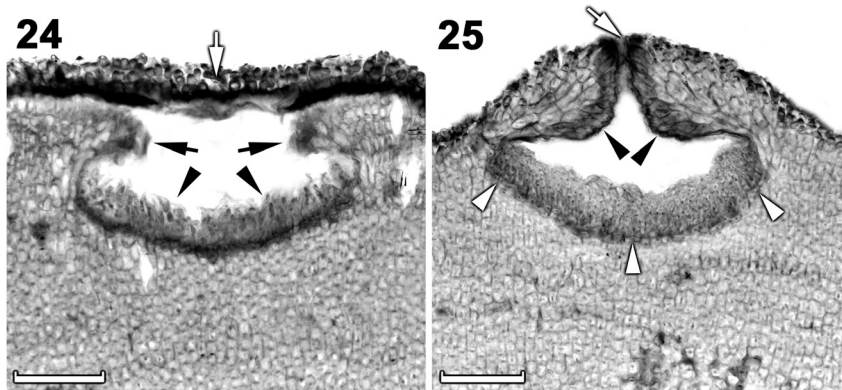
Thalli were dorsiventrally organized, monomerous and haustoria were absent. The medulla was thin and plumose (non-coaxial) (Figures 21, 22). Medullary filaments comprised rectangular to elongate cells, which gave rise to cortical filaments that comprised square to rectangular cells (Figures 22, 23). Contiguous medullary and cortical filaments were joined by cell fusions; secondary pit

connections were absent (Figures 22, 23). Subepithallial initials (intercalary meristematic cells) were square to rectangular (Figure 23). The epithallus was single layered with rounded to elliptical cells (Figure 23). Trichocytes were not observed. Data on morphological and measured vegetative characters are summarized in Table 1.

Reproductive morphology and anatomy: Gametangial thalli appeared to be dioecious, although female plants were not observed.

Spermatangial (male) conceptacles were uniporate, low-domed, raised above surrounding thallus surface (Figures 24, 25). Conceptacle chambers were transversely elliptical to flatten with the roof nearly twice as thick along the pore canal (Figure 25). The roof was formed from filaments peripheral to the fertile area (Figure 24). Throughout the early development, a protective layer of epithallial cells surrounded the conceptacle primordium (Figure 24). This protective layer was shed once the pore canal was near fully developed. The pore opening was occluded by a mucilage plug (Figure 25). In mature conceptacles the terminal initials along the pore canal were enlarged and papillate, they projected into the pore canal and were orientated more or less parallel to the conceptacle roof surface (Figure 25). Unbranched (simple) spermatangial systems were confined to floor of mature conceptacle (Figures 24, 25). Senescent male conceptacles appeared to be shed as no buried conceptacles were observed.

Tetrasporangial thalli were morphologically similar to spermatangial thalli. Conceptacles were uniporate, low domed and raised above surrounding the thallus surface (Figures 26–29). Conceptacle chambers were transversely elliptical to bean-shaped. The roof was nearly twice as thick along the pore canal and were 4–8 (9) cells (including an epithallial cell) thick (Figure 29). The pore canal tapered towards the surface was lined by elongated papillate cells that projected into the pore canal and were orientated more or less parallel or nearly perpendicular to the conceptacle roof surface (Figure 30). The roof was formed from filaments peripheral to the fertile area (Figures 26–28) and terminal initials were more elongate than their inward derivatives (Figure 27). Throughout the early development a protective layer of epithallial cells surrounded the conceptacle primordium (Figures 26–28). This protective layer was shed once the pore canal was near fully developed. The pore opening in mature conceptacles was unoccluded (Figures 29, 30). Throughout the development of the immature tetrasporangial conceptacle, a prominent columella of sterile filaments formed at the center of the conceptacle chamber (Figures 27, 28), which extended into the pore canal (Figure 29); the central columella appeared weakly calcified as with maturity it disintegrated to form a



Figures 24–25: Vertical section through the outer thallus showing spermatangial conceptacle primordium with peripheral roof development (black arrows) and simple spermatangial systems (black arrowheads) confined to the conceptacle floor. Note the protective layer of epithallial cells (white arrow). Scale bar = 50 µm. Vertical section through the outer thallus showing a mature, raised spermatangial conceptacle with the mucilage plug (white arrow) that occludes the pore opening and simple, spermatangial systems (white arrowheads) confined to the conceptacle floor. Note that the pore canal is lined with terminal, elongate initials (black arrowheads) that project into the pore canal as papillae. Scale bar = 50 µm.

low mound. The base of the pore canal was sunken into the chamber and terminal initials near the base pointed downward (Figures 29, 30). Mature conceptacle floors were sunken 11–24 cells (including the epithallial cell) below the surrounding thallus surface. Zonately divided tetrasporangia at maturity were arranged at the extreme periphery of conceptacle chamber and was attached via a stalk cell (Figure 29). Senescent tetrasporangial conceptacles appeared to be shed as no buried conceptacles were observed. Data on reproductive characters are summarized in Table 2.

Distribution: Confirmed by DNA sequences to have a wide, but disjunct distribution along the west coast, occurring from Port Nolloth to Groenriviermond (Northern Cape Province, ±220 km distance) and then from Cape St. Martin to Slangkop (Western Cape Province, ±200 km distance), South Africa.

***Chamberlainium occidentale* Puckree-Padua, P.W. Gabrielson et Maneveldt sp. nov.** (Figures 6, 31–35, 36–41, 42–46; Tables 1, 2).

Holotype: L 3986120, 01.x.2015, *leg. G.W. Maneveldt and C.A. Puckree-Padua*, collection number 15/61B, epilithic on primary bedrock in low intertidal zone.

Isotypes: UWC 15/58, UWC 15/59, UWC 15/61A

Type locality: South Africa, Western Cape Province, Lamberts Bay (32°6.5728' S, 18°18.1270' E).

Etymology: ‘*occidentale*’ from ‘*occidentalis*’, meaning western (Stearn 1973), making reference to the species’ wide-spread distribution along the west coast of Southern Africa.

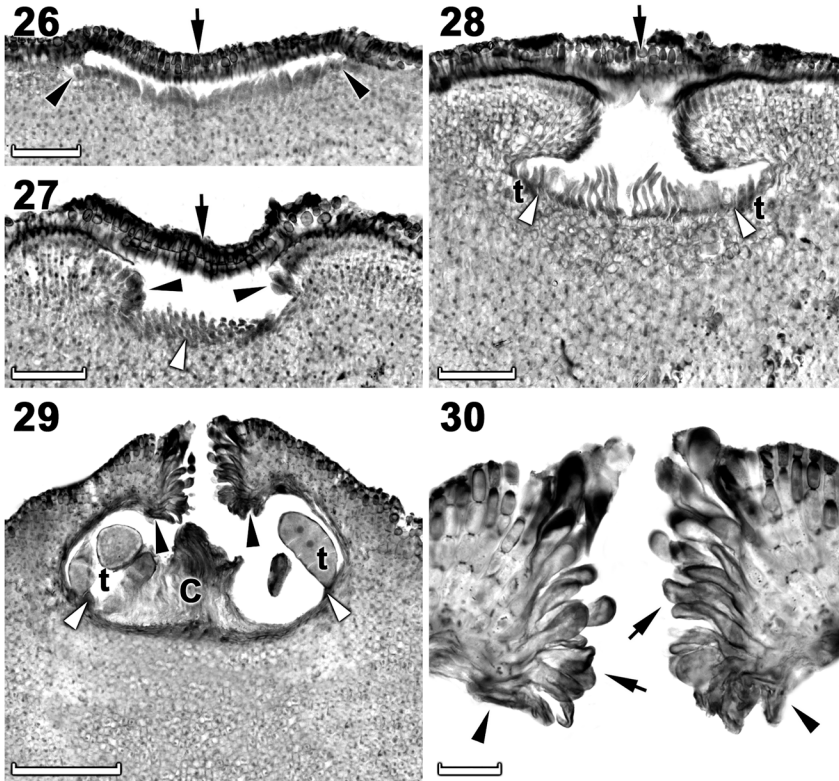
Description: Non-geniculate, thalli are variably thin to thick (up to 1000 µm), encrusting (smooth) to warty (mostly) to lumpy, becoming only slightly protuberant. Thalli are epilithic to epizoic and brownish beige in well-lit conditions. Individual crusts do not appear to coalesce (do

not fuse together) and are easily discernible. The thallus construction is monomerous with a single layer of epithallial cells. A central columella is present in tetrasporangial conceptacles, which persists to maturity. The pore opening in mature tetrasporangial conceptacles is unoccluded and slightly sunken below the surrounding roof surface. The *psbA* (851 bp) and *rbcL* (691–1,384 bp) sequences are diagnostic.

Habitat: Thalli were epilithic on the primary bedrock in the high, mid- and low intertidal zones and epizoic on mollusc shells in the low intertidal zone.

Vegetative morphology and anatomy: Plants were non-geniculate, thalli were variably thin to thick (up to 1000 µm), encrusting (smooth) to warty (mostly) to lumpy, becoming only slightly protuberant (protuberances 4 mm in height) (Figures 6, 31). Thalli were firmly adherent, brownish beige (in well-lit conditions) (Figures 6) to blue-gray to rosy pink (in dim light) when freshly collected. Individual crusts did not coalesce (did not fuse together) and were easily discernible (Figure 31).

Thalli were dorsiventrally organized, monomerous and haustoria were absent. The medulla was thin and plumose (non-coaxial) (Figures 32, 33). Medullary filaments comprised square to elongate cells, which gave rise to cortical filaments that comprised square to rectangular cells (Figures 33, 34). Contiguous medullary and cortical filaments were joined by cell fusions; secondary pit connections were absent (Figures 33, 34). Subepithallial initials were square to rectangular (Figure 35). The epithallus was single layered with elliptical to round to elongate cells (Figure 35). Trichocytes were common, mostly singularly, but also in clusters of up to 6 cells, separated by normal vegetative filaments (Figure 35). Trichocytes were always



Figures 26–30: *Chamberlainium glebosum* tetrasporangial anatomy. (26) Vertical section through the outer thallus showing an early stage tetrasporangial conceptacle primordium with peripherally arranged tetrasporangial initials (black arrowheads) and a protective layer of epithallial cells (black arrow) (UWC 15/17). Scale bar = 50 μ m. (27) Vertical section through the outer thallus showing a later stage tetrasporangial conceptacle primordium with peripheral roof development (black arrowheads) with a developing central columella (white arrowhead). Note the persisting layer of protective epithallial cells (black arrow) (UWC 15/17). Scale bar = 50 μ m. (28) Vertical section through a maturing tetrasporangial conceptacle showing tetrasporangial initials (t) arranged peripherally around a central columella (between white arrowheads). Note the layer of protective epithallial cells (black arrow) being shed (L 3986123). Scale bar = 50 μ m. (29) Vertical section through a mature, raised tetrasporangial conceptacle showing tetrasporangia (t) with stalk cells (white arrowheads), peripherally arranged around a well-defined central columella (C). Note the base of the pore canal sunken into the chamber with terminal, elongate initials near the base pointing downward (black arrowheads) (UWC 15/55). Scale bar = 100 μ m. (30) Magnified view of the pore canal of a mature tetrasporangial conceptacle showing terminal, elongate initials (black arrows) that project into the pore canal as papillae and the base of the pore canal sunken (black arrowheads) into the chamber with terminal, elongate initials near the base pointing downward (UWC 15/55). Scale bar = 20 μ m.

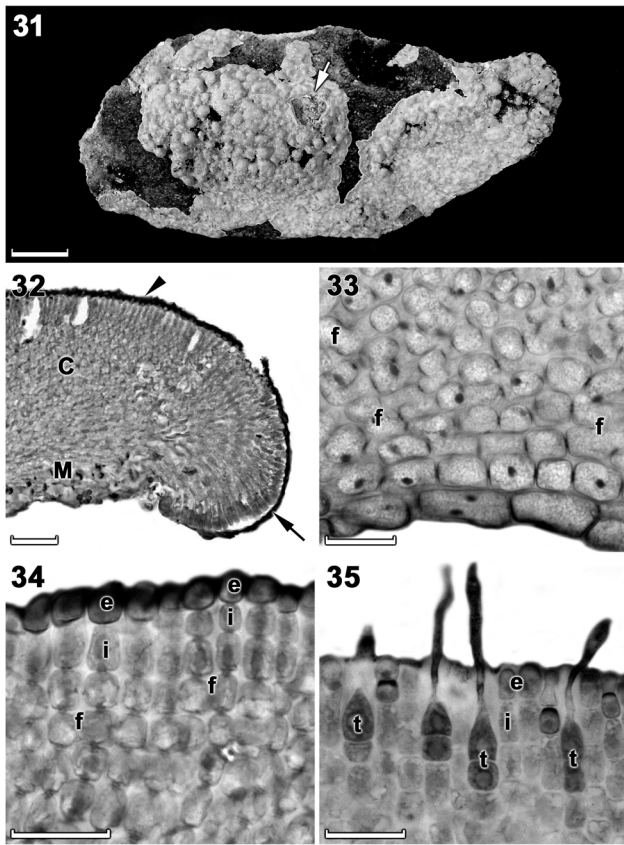
terminal and never intercalary in the cortex; buried trichocytes were not observed. Data on morphological and measured vegetative characters are summarized in Table 1.

Reproductive morphology and anatomy: Gametangial thalli were dioecious and monoecious. The type specimen bore all (including tetrasporangial) life cycle stages.

Spermatangial (male) conceptacles were uniporate, low-domed, and raised above surrounding thallus surface (Figures 36, 37). Conceptacle chambers were transversely elliptical to flatten and the roof nearly twice as thick along the pore canal (Figures 37, 38). The roof was formed from filaments peripheral to the fertile area (Figure 36). Throughout the early development, a protective layer of epithallial cells surrounded the conceptacle primordium (Figure 36). This protective layer was shed once the pore

canal was near fully developed. The pore opening was occluded by a mucilage plug (Figure 37). In mature conceptacles terminal initials along the pore canal were enlarged and papillate, they projected into the pore canal and were orientated more or less parallel to the conceptacle roof surface (Figure 38). Unbranched (simple) spermatangial systems were confined to the floor of the mature conceptacle (Figures 36, 37). Senescent male conceptacles appeared to be shed as no buried conceptacles were observed.

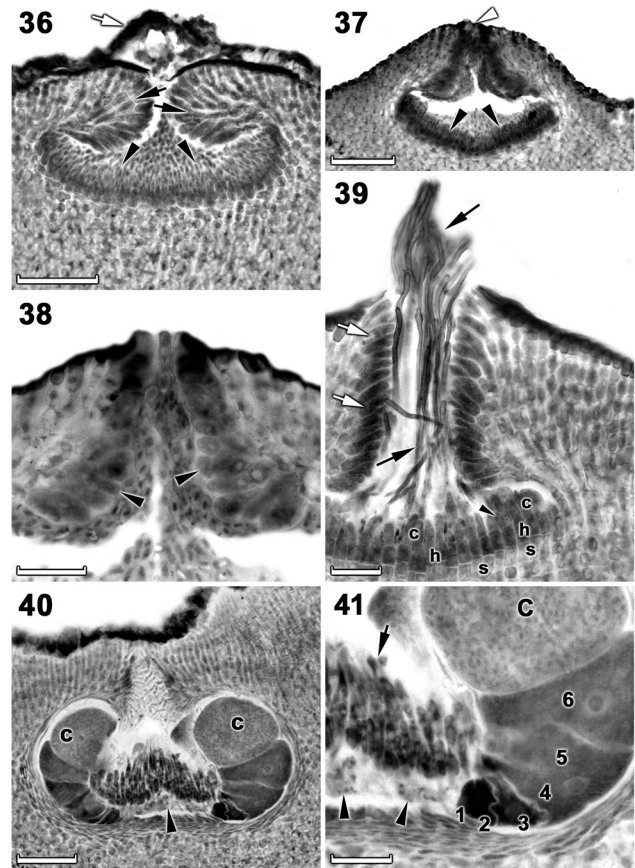
Carpogonial (female) conceptacles were similar in size and shape to spermatangial conceptacles and were raised above surrounding thallus surface (Figure 39). In mature conceptacles the terminal initials along the pore canal were enlarged and papillate, they projected into the pore canal and were orientated more or less parallel or nearly



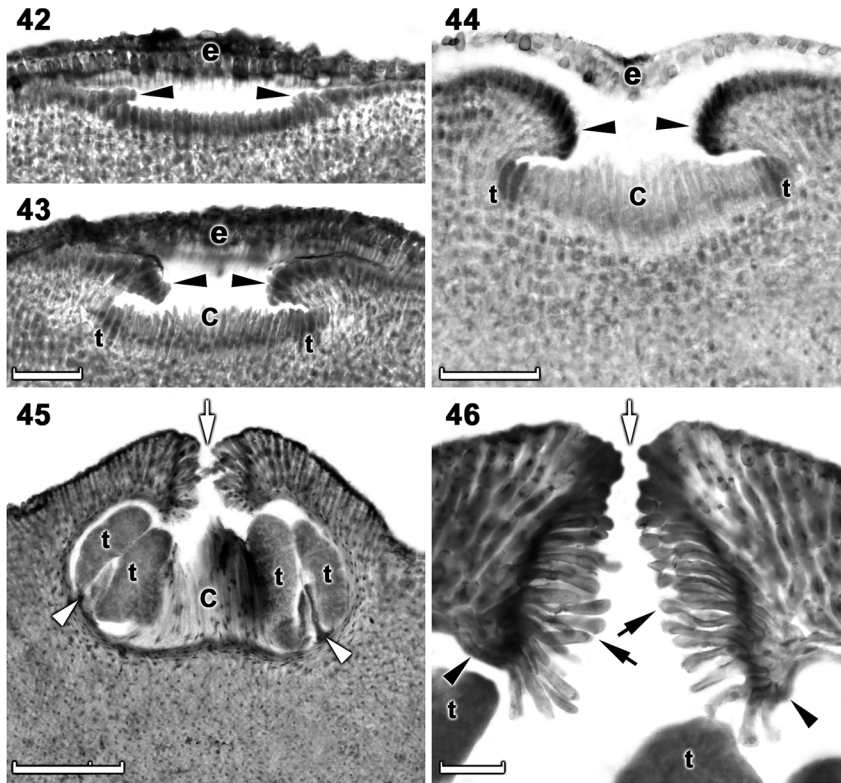
Figures 31–35: *Chamberlainium occidentale* habit and vegetative anatomy. (31) Rock fragment with holotype specimen showing the region (white arrow) of the holotype from which all analyses were done (L 3986120, gametangial and tetrasporangial). Scale bar = 10 mm. (32) Vertical section through the margin (black arrow) showing the monomerous thallus construction with plumose medulla (M) giving rise to cortical filaments (C) that terminate in a single layer of epithallial cells (black arrowhead) (UWC 15/59). Scale bar = 50 μ m. (33) Vertical section of the inner thallus showing cell fusions (f) between adjacent medullary filaments (UWC 15/56). Scale bar = 20 μ m. (34) Vertical section of the outer thallus showing a single layer of epithallial cells (e) subtended by a layer of subepithallial initials (i). Note the cell fusions (f) between adjacent cortical filaments (UWC 15/59). Scale bar = 20 μ m. (35) Vertical section of the outer thallus showing a single layer of epithallial cells (e) subtended by a layer of subepithallial initials (i). Note a cluster of bottle-shaped trichocytes (t) each separated by vegetative filaments (UWC 15/59). Scale bar = 20 μ m.

perpendicular to the conceptacle roof surface (Figure 39). Carposporangial branches developed across the floor of the conceptacle chamber, comprising a single support cell, a hypogynous cell and a carposporangium that extended into a trichogyne (Figure 39). Sterile cells were occasionally present on hypogynous cells (Figure 39).

After presumed karyogamy, carposporophytes developed within female conceptacles and formed carposporangial conceptacles (Figure 40). Carposporangial



Figures 36–41: *Chamberlainium occidentale* gametangial anatomy. (36) Vertical section through the outer thallus showing a spermatangial conceptacle primordium with peripheral roof development (black arrows) and simple spermatangial systems (black arrowheads) confined to the conceptacle floor. Note the protective layer of epithallial cells (white arrow) (L 3986120). Scale bar = 50 μ m. (37) Vertical section through a mature, raised spermatangial conceptacle showing the mucilage plug (white arrowhead) that occludes the pore opening and simple, spermatangial systems (black arrowheads) confined to the conceptacle floor (UWC 15/56). Scale bar = 50 μ m. (38) Magnified view through a mature spermatangial conceptacle showing the pore canal lined with terminal, elongate initials (black arrowheads) that project into the pore canal as papillae (UWC 15/56). Scale bar = 20 μ m. (39) Magnified view of a mature carposporangial conceptacle with carposporangial branches comprising a single support cell (s), a hypogynous cell (h) with sterile cell (black arrowhead), and a carposporangium (c) extended into a trichogyne (black arrows) that may project out of the pore. Note that the pore canal is lined with terminal, elongate initials (white arrows) that project into the pore canal as papillae (L 3986120). Scale bar = 20 μ m. (40) Vertical section through a mature carposporangial conceptacle showing a discontinuous central fusion cell (black arrowhead) with peripherally arranged gonimoblast filaments each terminating in a carposporangium (C) (L 3986120). Scale bar = 50 μ m. (41) Magnified view of the floor of a carposporangial conceptacle showing a discontinuous central fusion cell (black arrowheads) bearing a peripherally arranged gonimoblast filament (1–6) terminating in a carposporangium (C). The remains of unfertilised carposporangial branches (black arrow) persist across the dorsal surface of the central fusion cell (L 3986120). Scale bar = 20 μ m.



Figures 42–46: *Chamberlainium occidentale* tetrasporangial anatomy. (42) Vertical section through the outer thallus showing an early stage tetrasporangial conceptacle primordium with peripheral roof development (black arrowheads) and a protective layer of epithallial cells (e) (L 3986120). Scale bar = 50 µm. (43) Vertical section through the outer thallus showing a later stage tetrasporangial conceptacle primordium with peripheral roof development (black arrowheads) and tetrasporangial (t) initials arranged peripherally around a central columella (c). Note the persisting layer of protective epithallial cells (e) (UWC 93/220). Scale bar = 50 µm. (44) Vertical section through the outer thallus showing a maturing tetrasporangial conceptacle with peripheral roof development (black arrowheads) and tetrasporangial (t) initials, peripherally arranged around a central columella (c). Note the layer of protective epithallial cells (e) (UWC 93/220). Scale bar = 50 µm. (45) Vertical section through a mature, raised tetrasporangial conceptacle showing tetrasporangia (t) with stalk cells (white arrowheads), peripherally arranged around a well-defined central columella (C). Note, the sunken and unoccluded pore opening (white arrow) (UWC 93/220). Scale bar = 100 µm. (46) Magnified view of the pore canal of a mature tetrasporangial conceptacle showing terminal, elongate initials (black arrows) that project into the pore canal as papillae and the base of the pore canal sunken (black arrowheads) into the chamber with terminal, elongate initials near the base pointing downward. Note, the sunken and unoccluded pore opening (white arrow) (UWC 93/220). Scale bar = 20 µm.

conceptacles were comparatively large, low-domed, and raised above the surrounding thallus surface. Conceptacle chambers were transversely elliptical with flattened bottoms presumably caused by the growth of the gonimoblast filaments. Pore canals tapered towards the surface, were lined by enlarged papillate cells that projected into the pore canal and were orientated more or less parallel to the conceptacle roof surface (Figure 40). In mature conceptacles, the cells lining the pore canal were more elongate than their inward derivatives. The base of the pore canal was sunken into the chamber and terminal initials near the base characteristically pointed downward (Figure 40). A discontinuous central fusion cell was present and 5–7 celled gonimoblast filaments (including a terminal carposporangium) developed along the

periphery of the conceptacle chamber (Figures 40, 41). The remains of unfertilized carpogonia persisted across the dorsal surface of the fusion cell (Figures 40, 41). Senescent carposporangial conceptacles appeared to be shed as no buried conceptacles were observed.

Tetrasporangial thalli are morphologically similar to gametangial thalli. Conceptacles were uniporate, low domed and raised above the surrounding thallus surface (Figures 42–45). Conceptacle chambers were transversely elliptical to bean-shaped. The roof was nearly twice as thick along the pore canal and was 5–7 cells (including an epithallial cell) thick. The pore canal tapered towards the surface and was arched (Figure 46). The pore canal was lined by elongated papillate cells that projected into the pore canal and were orientated more or less parallel or nearly

perpendicular to the conceptacle roof surface (Figure 46). The roof was formed from filaments peripheral to the fertile area and terminal initials were more elongate than their inward derivatives (Figures 42–44). Throughout the early development a protective layer of epithallial cells surrounded the conceptacle primordium (Figures 42–44). This protective layer was shed once the pore canal was near fully developed. The pore opening was unoccluded and became slightly sunken below the surrounding roof surface (Figures 45, 46). Throughout development of the immature tetrasporangial conceptacle a prominent columella of sterile filaments formed at the center of the conceptacle chamber (Figures 43, 44), which persisted to maturity (Figure 45). The base of the pore canal was sunken into the chamber and terminal initials near the base point downward (Figure 46). Mature conceptacle floors were sunken 14–19 cells (including the epithallial cell) below the surrounding thallus surface. Zonately divided tetrasporangia at maturity were arranged at the extreme periphery of the conceptacle chamber and were attached via a stalk cell (Figure 45). Senescent tetrasporangial conceptacles appeared to be shed as no buried conceptacles were observed. Data on reproductive characters summarized in Table 2.

Distribution: Confirmed by DNA sequences to be widely distributed ($\pm 1,200$ km distance) along the west and southern west coasts, occurring from Lüderitz (Namibia) to Holbaaipunt (Western Cape Province), South Africa. The species is disjunct in the southern part of its range of ± 240 km.

4 Discussion

4.1 Subfamily and generic assignment

Puckree-Padua et al. (2020b) noted that there were no diagnostic characters that segregated the Corallinales subfamilies Chamberlainoideae, Corallinoideae or Neogoniolithoideae, and they also argued that it was premature to raise these subfamilies to the rank of family. Thus, taxa are assigned to these subfamilies based on DNA sequences of the commonly used markers for coralline systematics, nuclear encoded SSU or LSU and/or plastid encoded *psbA* or *rbcl*. Herein we used *psbA* and *rbcl* sequences to place three South African species in Chamberlainoideae, all of which were passing earlier under the name *S. yendoii*. Caragnano et al. (2018) proposed two morpho-anatomical characters to segregate *Spongites* (Neogoniolithoideae) from *Chamberlainium* (Chamberlainoideae): 1) diameter of tetra/bisporangial conceptacle

chambers (<300 μm for *Chamberlainium* and >300 μm for *Spongites*); and 2) number of cell layers composing roofs of tetra/bisporangial conceptacles (≤ 8 cell layers for *Chamberlainium* and >8 for *Spongites*). Neither of these characters is now useful to segregate these genera (Table 3). *Chamberlainium impar* (Puckree-Padua et al. 2020b) and *C. occidentale* (this study) both have conceptacle chamber diameters >300 μm (up to 365 μm). Additionally, *C. glebosum* has up to nine cell layers comprising tetrasporangial conceptacle roofs. The two genera recognized within Chamberlainoideae, *Chamberlainium* and *Pneophyllum* are still segregated by their different types of tetrasporangial conceptacle roof development, type 1 or SUR-type (from filaments surrounding the fertile area) in the former versus type 2 or COL-type (from filaments surrounding and within the fertile area) in the latter (see also Johansen 1976; Townsend 1981). Based on a combination of DNA sequences and tetrasporangial conceptacle roof development, we were able to correctly assign South African species previously placed in *Spongites* in either *Chamberlainium* (Puckree-Padua et al. 2020b, this study) or *Pneophyllum* (Puckree-Padua et al. 2020a). The generic assignment of New Zealand species previously placed in *S. yendoii* by Broom et al. (2008), which represent multiple distinct species (Sissini et al. 2014), as well as topotype material of *S. yendoii* from Japan, needs to be reassessed.

For Chamberlainoideae Caragnano et al. (2018) reported trichocytes to be absent or present; when present, occurring singly or paired, but always terminal and never intercalary in the perithallus (cortex). However, our research has shown that for *C. cochleare*, *C. natalense* (Puckree-Padua et al. 2020b), and *C. occidentale* (this study) trichocytes can occasionally occur in horizontal clusters of up to six cells, but each trichocyte is separated by one or more vegetative filaments (Table 3). Although this arrangement differs from that characteristic of Porolithoideae, where trichocytes are tightly packed in horizontal fields without any vegetative filaments between them (Kato et al. 2011), it is inconsistent with the description of Chamberlainoideae proposed by Caragnano et al. (2018). Additionally, Caragnano et al. (2018) proposed that trichocyte development in *Chamberlainium* was of the *Jania rubens* type (Cabioch 1971; Johansen 1981). Observations of *C. decipiens* (van der Merwe et al. 2015), *C. cochleare*, *C. impar*, *C. natalense* (Puckree-Padua et al. 2020b), *C. capense* and *C. occidentale*, suggest that trichocyte development in *Chamberlainium* is rather of the *Fosliella* type. Here the overlying epithallial cell is shed prior to the trichome elongation and final development (Johansen 1981: 34, fig. 18); in the *J. rubens* type of development the epithallial cell is not shed and instead the trichome

Table 3: Morpho-anatomical characters considered by Caragnano et al. (2018) to be informative in distinguishing among *Chamberlainium*, *Pneophyllum* and *Spongites* and the corresponding characters subsequently established for these taxa in South Africa.

| Character | <i>Chamberlainium</i> (Caragnano et al. 2018) | <i>Chamberlainium</i> (Puckree-Padua et al. 2020b, this study) | <i>Pneophyllum</i> (Caragnano et al. 2018) | <i>Pneophyllum</i> (Puckree-Padua et al. 2020a) | <i>Spongites</i> (Caragnano et al. 2018) |
|---|--|--|--|--|---|
| Thallus thickness | <1 mm | ≤2 mm | Generally <200 μm, or filaments up to 20 cells | <1 mm (primary thalli), ≤3 mm (secondary thalli) | Up to several mm |
| Thallus construction | Dimerous or monomeric, but not both | Dimerous or monomeric, but not both | Dimerous | Primarily dimerous, becoming secondarily monomeric | Dimerous or monomeric (can be both) |
| No. of epithallial cells | 1–4 | 1–6 (9) | 1 | 1–4 | 1–3 |
| Trichocyte arrangement (when present) | Solitary, paired (never in horizontal rows) | Solitary, paired, clustered in horizontal fields but separated by vegetative filaments | Solitary, paired | None observed | Solitary, horizontal fields, vertical rows |
| Development of tetra/bisporangial conceptacle roof | Type 1 | Type 1 | Type 2 | Type 2 | Type 1 |
| Diameter of tetra/bisporangial conceptacle chambers | <300 μm | Up to 365 μm | <350 μm | <350 μm | >300 μm |
| No. of tetra/bisporangial conceptacle roof cells | ≤8 | ≤8 (9) | <8 | Up to 22 | >8 |
| Central columella present/absent in tetra/bisporangial conceptacle chambers | Absent or present | Present, but may disintegrate with maturity | Absent or present | Present, but may disintegrate with maturity | Present, poorly developed |
| Distribution of tetra/bisporangial in tetra/bisporangial conceptacle chambers | Peripheral or across chamber floor | Peripheral, but may appear across the chamber floor as central columella disintegrates | Peripheral | Peripheral | Peripheral |

develops to project through the epithallial layer (Judson and Poeschel 2002). These contradictory examples suggest that the characterization of *Chamberlainium* (and possibly also *Pneophyllum*, see Puckree-Padua et al. 2020a) will need emending. We propose that any emendation should avoid including characters that are either highly variable, or are difficult to interpret.

4.2 Species relationships

The interspecific sequence divergence values from the *psbA* and *rbcL* genes indicate that *C. capense*, *C. glebosum* and *C. occidentale* are distinct species (Tables S2, S3). This is supported by the ABDG analysis reported in Puckree-Padua et al. (2020b). These species occur in a fully supported clade in analyses of both the *psbA* and *rbcL* genes, although the relationships among the species are unresolved. Both Bayesian and ML analyses of *rbcL* sequences fully support *C. capense* sister to *C. occidentale*, whereas

the same analyses of *psbA* sequences moderately supports *C. capense* sister to *C. glebosum*. The overall distributions of these three South African nearly endemic species overlap – *C. occidentale* extends north into southern Namibia (Figure 1) – but each has unique ranges (discussed below). The analyses of both genes also moderately (*psbA*) to strongly (*rbcL*) support another endemic South African species, *C. cochleare*, as sister to these three species. However, *C. cochleare* is distributed further east along the south coast and does not overlap the ranges of *C. capense*, *C. glebosum* and *C. occidentale*. The phylogenetic relationships of these four species with the three other named South African *Chamberlainium* species, *C. agulhense*, *C. impar* and *C. natalense* and with the NE Pacific species *C. tumidum* and *C. decipiens*, are unresolved in the *rbcL* tree (Figure 3), whereas in the *psbA* tree, *C. agulhense*, *C. impar* and *C. natalense* are moderately to strongly supported as sister to two unnamed *Chamberlainium* species. Analysis of additional markers, such as LSU, SSU or CO1 may be helpful in resolving this relationships.

4.3 Species accounts

Collectively, the geographic distributions, substrate, habit, habitat, growth form and color of living thalli are useful characters for field identification of the various South African species of *Chamberlainium* thus far described (Table 4). Of the named *Chamberlainium* species, *C. agulhense* has the most restricted distribution, occurring epilithically on the primary bedrock mostly in the high intertidal along the South African warm temperate south coast (Benguela-Agulhas Transition Zone; Smit et al. 2017) within a narrow 10 km range (van der Merwe et al. 2015). *Chamberlainium cochleare* and *C. natalense* have wide distributional ranges, but are restricted to the warm temperate south coast (Benguela-Agulhas Transition Zone and the Agulhas Marine Province; Smit et al. 2017) and subtropical east coast (East Coast Transition Zone; Smit et al. 2017) (Puckree-Padua et al. 2020b). *Chamberlainium cochleare* is epilithic on the primary bedrock in the mid to low intertidal zone and is characteristically associated with the gardening limpet, *Scutellastra cochlear*, whereas, *C. natalense* is found largely epilithic on boulders in intertidal rock pools. *Chamberlainium capense*, *C. impar*, *C. glebosum* and *C. occidentale* are all largely cold temperate species restricted to the cool temperate west coast (Benguela Marine Province; Smit et al. 2017) (Puckree-Padua et al. 2020, this study). Along this coast *C. capense* (± 43 km) and *C. impar* (± 170 km) have restricted southerly distributions and are epilithic in the mid to low intertidal zone. *Chamberlainium glebosum* has a wide, but disjunct distribution (± 220 and ± 200 km) with a gap north and south of Lambert's Bay. The species is epilithic on the primary bedrock throughout the intertidal zone. Similar to *C. cochleare* and *C. natalense*, *C. occidentale* has a wide distribution ($\pm 1,200$ km) along the African southern west coast occurring on bedrock throughout the intertidal zone and epizoid on the shells of live molluscs; the species has a disjunction in the southern part of its range of ± 240 km. While gross morphology (growth form and thallus color) is a useful character for separating taxa across biogeographic boundaries (the warm temperate and subtropical species are generally encrusting to smooth; the cool temperate species are generally warty to lumpy, becoming highly protuberant), it is not useful within biogeographic regions. *Chamberlainium impar*, however, has a unique yellowish to yellow-brown thallus that is pachydermatous and often highly confluent. Of all the species *C. cochleare* is the only one in which individual thalli are not discernible due to their fusing to form large expanses.

Aside from these collective field characters, histological examination in the laboratory has shown that thallus construction, trichocyte arrangement, number of epithallial cell layers and the structure of the tetrasporangial conceptacle pore canal are useful anatomical characters (Table 4) to distinguish some species. *Chamberlainium agulhense* is the only dimerous species. While trichocytes have not been observed in *C. agulhense* and *C. glebosum*, they occurred singly to paired in *C. capense* and *C. impar*, and often occurred clustered in small horizontal fields in *C. cochleare*, *C. natalense* and *C. occidentale*. Most species have only a single layer of epithallial cells, but *C. agulhense* can have up to 3 layers of epithallial cells; *C. impar* is always multi-layered with up to 9 layers of epithallial cells. The tetrasporangial conceptacle pore is not occluded in *C. agulhense*, *C. glebosum* and *C. occidentale*, although in the last species the pore opening is slightly sunken below the surrounding roof. The projecting corona above the tetrasporangial conceptacle pore may be useful for distinguishing *C. capense* from all other South African species of *Chamberlainium* except for *C. natalense* (Puckree-Padua et al. 2020b). As in *C. natalense*, the corona appears to develop from filaments near the upper half of the tetrasporangial conceptacle roof, directly adjacent to the pore canal. However, *C. natalense* is mostly found on boulders and pebbles in rock pools and has a thinner thallus (up to 800 μm) that is entirely smooth (lacking protuberances). Moreover the two species do not have overlapping distributions with *C. capense* found in cool temperature waters whereas *C. natalense* is found in warm temperate to subtropical waters. In *C. cochleare* and *C. impar*, the tetrasporangial conceptacle pore is occluded by a mucilage plug, but the two species are morphologically distinct (Table 4). Except for the corona of filaments that occlude the tetrasporangial conceptacle pore in *C. capense*, anatomically there are no useful, observable characters with a light microscope that separate this species from either *C. glebosum* or *C. occidentale*. However, of all the South African *Chamberlainium* species thus far described, *C. glebosum* is the most protuberant.

4.4 Range-restricted coralline endemics

For most marine algae, range-restrictions seem to be associated with biogeographic boundaries or transition zones (Anderson et al. 2009; Montecinos et al. 2012). While the underlying mechanisms that result in coralline algal range-restrictions remain unknown (Hind et al. 2016), biogeographic breaks offer a plausible explanation for some species. There are now several examples of coralline

Table 4: Features found to be informative for distinguishing among the various South African species of *Chamberlainium* thus far described.

| Character | <i>Chamberlainium agulhense</i> (van der Merwe et al. 2015) | <i>Chamberlainium capense</i> (this study) | <i>Chamberlainium cochleare</i> (Puckree-Padua et al. 2020b) | <i>Chamberlainium glebosum</i> (this study) | <i>Chamberlainium impar</i> (Puckree-Padua et al. 2020b) | <i>Chamberlainium natalense</i> (Puckree-Padua et al. 2020b) | <i>Chamberlainium occidentale</i> (this study) |
|---|--|--|---|---|---|--|---|
| Endemic | Yes | Yes | Yes | Yes | Yes | Yes | No (Namibia and South Africa) |
| Geographical distribution | Restricted distribution (±10 km) along the southern west coast | Restricted distribution (±43 km) along the southern west coast | Widely distributed (±1,700 km) along the southern and eastern coasts | Disjunct distribution (±220 and ±200 km) along the west coast | Restricted distribution (±170 km) along the southern west coast | Widely distributed (±1,720 km) along the southern west and eastern coasts | Widely distributed (±1,200 km) along the west and southern west coasts |
| Substrate | Epilithic on bedrock | Epilithic on bedrock and boulders; epizoic on mollusc shells | Epilithic on bedrock; epizoic on mollusc shells, especially <i>S. cochlear</i> | Epilithic on bedrock | Epilithic on bedrock | Largely epilithic on boulders and pebbles; occasionally epilithic on bedrock; epizoic on winkle shells | Epilithic on bedrock; epizoic on mollusc shells |
| Habitat | High (mostly) to mid-intertidal (rock pools mostly) to low intertidal. | Mid-intertidal (rock pools mostly) to low intertidal. | Mid- to low intertidal. | High to mid-shore (mostly) to occasionally on the low shore. | Mid- to low intertidal. | Mid- to low intertidal rock pools. | High to low (largely) intertidal |
| Growth form | Encrusting (smooth) | Encrusting (smooth), becoming variably lumpy (mostly) and slightly protuberant | Encrusting (smooth) | Lumpy, becoming highly protuberant | Encrusting (smooth), orbicular becoming confluent | Encrusting (smooth) | Encrusting (smooth) to warty (mostly) to lumpy, becoming slightly protuberant |
| Habit | Individual thalli discernible, not fusing | Individual thalli discernible, not fusing | Individual thalli not discernible, fusing to form large expanses | Individual thalli discernible, not fusing | Individual thalli discernible, not fusing | Individual thalli discernible, not fusing | Individual thalli discernible, not fusing |
| Color of living thalli (in well-lit conditions) | Brownish-pink | Bright to dusky pink | Greyish | Brownish pink to gray | Yellowish to yellow brown | Blue-gray | Brownish beige |
| Thallus construction | Dimerous | Monomerous | Monomerous | Monomerous | Monomerous | Monomerous | Monomerous |
| Trichocyte arrangement | None observed | Common, solitary (mostly) to paired | Common, solitary (mostly) to clustered, up to 6 (separated by vegetative filaments) | None observed | Rare, solitary to paired | Rare, solitary (mostly) to clustered, up to 6 (separated by vegetative filaments) | Common, solitary (mostly) to clustered, up to 6 (separated by vegetative filaments) |
| No. of epithallial cell layers | 1–3 (mostly 1–2) | 1 | 1 | 1 | 4–6 (9) | 1 | 1 |
| Mature tetrasporangial pore characteristics | Pore opening unoccluded | Pore opening occluded by a corona of filaments | Pore opening occluded by a mucilage plug | Pore opening unoccluded | Pore opening occluded by a mucilage plug | Pore opening occluded by a corona of filaments | Pore opening unoccluded; pore slightly sunken below the surrounding roof |

algae with restricted geographical ranges (e.g., Hind et al. 2016; Pardo et al. 2014; Peña et al. 2014, 2015; Wilson et al. 2004), and South Africa is no exception, being bathed and influenced by three oceans, the western Atlantic (with its cold Benguela Current), the eastern Indian (with its warm Agulhas Current), and the Southern Ocean to the south (with its cold Antarctic Circumpolar Current). Due to their proximity, the former two ocean currents have the greatest influence on the South African marine biota. The effects of these ocean currents have resulted in two marine provinces and two biogeographic transition zones (Figure 1; see Smit et al. 2017). The western biogeographic transition zone (Benguela-Agulhas Transition Zone) is located within the Cape Peninsula and experiences rapid changes in temperature (Bolton and Anderson 1997; Leliaert et al. 2000; Smit et al. 2017). This biogeographic break seems to be largely responsible for the distributional ranges we observed for the South African species ascribed to *Chamberlainium* (Puckree-Padua et al. 2020b; van der Merwe et al. 2015, this study) and *Pneophyllum* (Puckree-Padua et al. 2020a). Within *Chamberlainium*, at least three species, *C. agulhense* (van der Merwe et al. 2015), *C. impar* (Puckree-Padua et al. 2020b), and *C. capense* (this study) have restricted geographic ranges, all of them associated with biogeographic boundaries or transition zones. *Chamberlainium agulhense* has the most restricted distribution (10 km range), occurring along the South African warm temperate south coast in the western biogeographic transition zone (Benguela-Agulhas Transition Zone; Smit et al. 2017) (van der Merwe et al. 2015). The precise reason for this very narrow range is unclear, but another non-geniculate coralline alga, *Heydrichia cerasina* Maneveldt et E. van der Merwe has the same biogeographic distribution (Maneveldt and van der Merwe 2012), suggesting that the Cape Agulhas region, where these species occur, represents a region of biogeographic interest. *Chamberlainium capense* (± 43 km) and *C. impar* (± 170 km) are both cool temperate species and are restricted to the southern regions of the Benguela Marine Province. The two species have a small overlap (± 4 km) in their northern and southern distributions respectively. Interestingly, *C. occidentale*, a cool temperate species with a wide distribution ($\pm 1,200$ km) along the African southern west coast, also has a disjunction in the southern part of its range of ± 240 km. *Chamberlainium glebosum* could also be considered a range-restricted endemic because within its disjunct distribution (± 220 and ± 200), the species appears to be restricted, with a gap north and south of Lambert's Bay.

5 Conclusions

DNA sequencing is profoundly changing our understanding of the composition of the South African non-geniculate coralline flora. Thus far, none of the species previously reported from South Africa based on morpho-anatomy, and whose type localities are on other continents, is correctly applied in South Africa, e.g., *P. discoideum* (as *S. discoideus*) from South America (Puckree-Padua et al. 2020a), *S. yendoi* from Japan (Puckree-Padua et al. 2020b), and *Phymatolithon repandum* from Australia (Maneveldt et al. 2020). Very likely none of the remaining 19 species, with their type localities on other continents, are present in South Africa (see Maneveldt et al. 2016 for the most recent list). In addition, seven distinct species were passing under *S. yendoi* in South Africa, none of them are that species, and all are classified in the recently erected genus, *Chamberlainium*. We have just scratched the surface sequencing DNA from only two genera, *Spongites* and *Phymatolithon*, of the 18 reported from South Africa (Maneveldt et al. 2016). We anticipate, with further research, finding many additional misapplied names and undescribed taxa.

Acknowledgments: We thank Wilson Freshwater, DNA Analysis Core Facility, University of North Carolina, Wilmington for providing sequencing support and Todd Vision for providing research space and equipment to PWG. We are grateful to Arley Muth for collecting material in Chile and to the Amsler lab (University of Alabama, Birmingham) for collecting material in Antarctica.

Author contributions: All the authors have accepted responsibility for the entire content of this submitted manuscript and approved submission.

Research funding: We thank the Department of Biodiversity and Conservation Biology at the University of the Western Cape for providing funding and research equipment. The South African National Research Foundation (NRF), the South African National Botanical Institute (SANBI) through its Foundational Biodiversity Information (FBIP) and SEAKEYS programmes, and the Department of Science and Technology (DST) through its African Coelacanth Ecosystem (ACEP) and Phuhlisa programmes, are thanked for research funding, bursaries and travel awards to GWM and CAP-P. PWG acknowledges a private family trust for research support.

Conflict of interest statement: The authors declare no conflicts of interest regarding this article.

References

- Adey, W.H. and Adey, P.J. (1973). Studies on the biosystematics and ecology of the epilithic crustose Corallinaceae of the British Isles. *Br. Phycol. J.* 8: 343–407.
- Anderson, R.J., Bolton, J.J., and Stegenga, H. (2009). Using the biogeographic distribution and diversity of seaweed species to test the efficacy of marine protected areas in the warm temperate Agulhas Marine Province, South Africa. *Divers. Distrib.* 15: 1017–1027.
- Bolton, J.J. and Anderson, R.J. (1997). Marine vegetation. In: Cowling, R.M., Richardson, D.M., and Pierce, S.M. (Eds.), *Vegetation of Southern Africa*. Cambridge University Press, pp. 348–370.
- Broom, J.E.S., Hart, D.R., Farr, T.J., Nelson, W.A., Neill, K.F., Harvey, A.S., and Woelkerling, W.J. (2008). Utility of *psbA* and *nSSU* for phylogenetic reconstruction in the Corallinales based on New Zealand taxa. *Mol. Phylogenet. Evol.* 46: 958–973.
- Cabioch, J. (1971). Essai d'une nouvelle classification des Corallinacées actuelles. *C. R. Acad. Sci. Paris, Série D* 272: 1616–1619.
- Caragnano, A., Foetisch, A., Maneveldt, G.W., Millet, L., Liu, L.C., Lin, S.M., Rodondi, G., and Payri, C.E. (2018). Revision of Corallinaceae (Corallinales, Rhodophyta): recognizing *Dawsoniolithon* gen. nov., *Parvicellularium* gen. nov. and Chamberlainoideae subfam. nov. containing *Chamberlainium* gen. nov. and *Pneophyllum*. *J. Phycol.* 54: 391–409.
- Chamberlain, Y.M.C. (1990). The genus *Leptophytum* (Rhodophyta, Corallinales) in the British Isles with descriptions of *Leptophytum bornetii*, *L. elatum* sp. nov. and *L. laevae*. *Br. Phycol. J.* 25: 179–199.
- Chamberlain, Y.M.C. (1993). Observations on the crustose coralline red alga *Spongites yendoii* (Foslie) comb. nov. in South Africa and its relationship to *S. decipiens* (Foslie) comb. nov. and *Lithophyllum natalense* Foslie. *Phycologia* 32: 100–115.
- Edgar, R.C. (2004). Muscle: multiple sequence alignment with high accuracy and high throughput. *Nucleic Acids Res.* 32: 1792–97.
- Gabrielson, P.W., Miller, K.A., and Martone, P.T. (2011). Morphometric and molecular analyses confirm two distinct species of *Calliarthron* (Corallinales, Rhodophyta), a genus endemic to the northeast Pacific. *Phycologia* 50: 298–316.
- Hind, K.R., Gabrielson, P.W., Jensen, C.P., and Martone, P.T. (2016). *Crusticorallina* gen. nov., a non-geniculate genus in the subfamily Corallinoideae (Corallinales, Rhodophyta). *J. Phycol.* 52: 929–941.
- Huelsenbeck, J.P. and Ronquist, F. (2001). MRBAYES: Bayesian inference of phylogenetic trees. *Bioinformatics* 17: 754–755.
- Hughey, J.R., Silva, P.C., and Hommersand, M.H. (2001). Solving taxonomic and nomenclatural problems in Pacific Gigartinaceae (Rhodophyta) using DNA from type material. *J. Phycol.* 37: 1091–1109.
- Jeong, S.Y., Nelson, W.A., Sutherland, J.E., Peña, V., Le Gall, L., Diaz-Pulido, G., Won, B.Y., and Cho, T.O. (2020) (in press). Corallinapetrales and Corallinapetraceae: a new order and family of coralline red algae including *Corallinapetra gabriellii* comb. nov. *J. Phycol.* <https://doi.org/10.1111/jpy.13115>.
- Johansen, H.W. (1976). Phycological reviews 4: current status of generic concepts in coralline algae (Rhodophyta). *Phycologia* 15: 221–244.
- Johansen, H.W. (1981). *Coralline algae, a first synthesis*. CRC Press, Boca Raton, Florida.
- Judson, B.L. and Pueschel, C.M. (2002). Ultrastructure of trichocyte (hair cell) complexes in *Jania adhaerens* (Corallinales, Rhodophyta). *Phycologia* 41: 68–78.
- Kato, A., Baba, M., and Suda, S. (2011). Revision of the Mastophoroideae (Corallinales, Rhodophyta) and polyphyly in nongeniculate species widely distributed on Pacific coral reefs. *J. Phycol.* 47: 662–72.
- Kearse, M., Moir, R., Wilson, A., Stones-Havas, S., Cheung, M., Sturrock, S., Buxton, S., Cooper, A., Markowitz, S., Duran, C., et al. (2012). Geneious Basic: an integrated and extendable desktop software platform for the organization and analysis of sequence data. *Bioinformatics* 28: 1647–1649.
- Keats, D.W., Groener, A., and Chamberlain, Y.M.C. (1993). Cell sloughing in the littoral zone coralline alga, *Spongites yendoii* (Foslie) Chamberlain (Corallinales, Rhodophyta). *Phycologia* 32: 143–150.
- Leliaert, F., Anderson, R.J., Bolton, J.J., and Coppejans, E. (2000). Subtidal understory algal community structure in kelp beds around the Cape Peninsula (Western Cape, South Africa). *Bot. Mar.* 43: 359–366.
- Maneveldt, G.W. and Keats, D.W. (2008). Effects of herbivore grazing on the physiognomy of the coralline alga *Spongites yendoii* and on associated competitive interactions. *Afr. J. Mar. Sci.* 30: 581–593.
- Maneveldt, G.W. and van der Merwe, E. (2012). *Heydrichia cerasina* sp. nov. (Sporolithales, Corallinophycidae, Rhodophyta) from the southern-most tip of Africa. *Phycologia* 51: 11–21.
- Maneveldt, G.W., Chamberlain, Y.M.C., and Keats, D.W. (2008). A catalogue with keys to the non-geniculate coralline algae (Corallinales, Rhodophyta) of South Africa. *South Afr. J. Bot.* 74: 555–566.
- Maneveldt, G.W., van der Merwe, E., and Keats, D.W. (2016). Updated keys to the non-geniculate coralline red algae (Corallinophycidae, Rhodophyta) of South Africa. *South Afr. J. Bot.* 106: 158–164.
- Maneveldt, G.W., Gabrielson, P.W., and Kangwe, J. (2017). *Sporolithon indopacificum* sp. nov. (Sporolithales, Rhodophyta) from tropical western Indian and western Pacific oceans: first report, confirmed by DNA sequence data, of a widely distributed species of *Sporolithon*. *Phytotaxa* 326: 115–128.
- Maneveldt, G.W., Jeong, S.Y., Cho, T.O., Hughey, J.R., and Gabrielson, P.W. (2020). Reassessment of misapplied names, *Phymatolithon ferox* and *P. repandum* (Hapalidiales, Corallinophycidae, Rhodophyta) in South Africa, based on DNA sequencing of type and recently collected material. *Phycologia* 59: 449–455.
- Montecinos, A., Broitman, B.R., Faugeron, S., Haye, P.A., Tellier, F., and Guillemain, M. (2012). Species replacement along a linear coastal habitat: phylogeography and speciation in the red alga *Mazzaella laminarioides* along the south east pacific. *BMC Evol. Biol.* 12: 97.
- Pardo, C., López, L., Peña, V., Hernández-Kantún, J., Le Gall, L., Bárbara, I., and Barreiro, R. (2014). A multilocus species delimitation reveals a striking number of species of coralline algae forming maërl in the OSPAR maritime area. *PLoS One* 9: e104073.

- Peña, V., Rousseau, F., De Reviers, B., and Le Gall, L. (2014). First assessment of the diversity of coralline species forming maërl and rhodoliths in Guadeloupe, Caribbean using an integrative systematic approach. *Phytotaxa* 190: 190–215.
- Peña, V., De Clerck, O., Afonso-Carrillo, J., Ballesteros, E., Bárbara, I., Barreiro, R., and Le Gall, L. (2015). An integrative systematic approach to species diversity and distribution in the genus *Mesophyllum* (Corallinales, Rhodophyta) in Atlantic and Mediterranean Europe. *Eur. J. Phycol.* 50: 1–15.
- Puckree-Padua, C.A., Gabrielson, P.W., Hughey, J.R., and Maneveldt, G.W. (2020a) (in press). DNA sequencing of type material reveals *Pneophyllum marlothii* comb. nov. from South Africa and *P. discoideum* comb. nov. (Chamberlainioideae, Corallinales, Rhodophyta) from Argentina. *J. Phycol.* <https://doi.org/10.1111/jpy.13047-20-081>.
- Puckree-Padua, C.A., Haywood, A., Gabrielson, P.W., and Maneveldt, G.W. (2020b) (in press). Reassignment of some South African species to *Chamberlainium*, with a comment about the recognition of families of Corallinales (Rhodophyta). *Phycologia* 59, <https://doi.org/10.1080/00318884.2020.1975797>.
- Rösler, A., Perfectti, F., Peña, V., and Braga, J.C. (2016). Phylogenetic relationships of Corallinaceae (Corallinales, Rhodophyta): taxonomic implications for reef-building corallines. *J. Phycol.* 52: 412–431.
- Sissini, M.N., Oliveira, M.C., Gabrielson, P.W., Robinson, N.M., Okolodkov, Y.B., Riosmena-Rodríguez, R., and Horta, P.A. (2014). *Mesophyllum erubescens* (Corallinales, Rhodophyta): so many species in one epithet. *Phytotaxa* 190: 299–319.
- Smit, A.J., Bolton, J.J., and Anderson, R.J. (2017). Seaweeds in two oceans: beta-diversity. *Frontiers Mar. Sci.* 4: 404.
- Stamatakis, A. (2006). RAxML-VI-HPC: maximum likelihood-based phylogenetic analyses with thousands of taxa and mixed models. *Bioinformatics* 22: 2688–2690.
- Stearn, W.T. (1973). *Botanical Latin*. David and Charles, Newton Abbot.
- Stephenson, T.A. and Stephenson, A. (1972). *Life between tidemarks on rocky shores*. Freeman, San Francisco.
- Thiers, B.M. (2020). [Continuously updated electronic resource]. Index herbariorum: a global directory of public herbaria and associated staff. New York Botanical Garden's Virtual Herbarium, Available at: <http://sweetgum.nybg.org/ih/>.
- Townsend, R.A. (1981). Tetrasporangial conceptacle development as a taxonomic character in the Mastophoroideae and Lithophylloideae (Rhodophyta). *Phycologia* 20: 407–414.
- van der Merwe, E., Miklasz, K., Channing, A., Maneveldt, G.W., and Gabrielson, P.W. (2015). DNA sequencing resolves species of Spongites (Corallinales, Rhodophyta) in the Northeast Pacific and South Africa, including *S. agulhensis* sp. nov. *Phycologia* 54: 471–90.
- Wilson, S., Blake, C., Berges, J.A., and Maggs, C.A. (2004). Environmental tolerances of free-living coralline algae (maërl): implications for European marine conservation. *Biol. Conserv.* 120: 279–289.
- Woelkerling, W.J., Irvine, L.M., and Harvey, A.S. (1993). Growth-forms in non-geniculate coralline red algae (Corallinales, Rhodophyta). *Aust. Syst. Bot.* 6: 277–293.

Supplementary Material: The online version of this article offers supplementary material (<https://doi.org/10.1515/bot-2020-0074>).

Bionotes



Courtney A. Puckree-Padua

Department of Biodiversity and Conservation Biology, University of the Western Cape, P. Bag X17, Bellville 7535, South Africa
<https://orcid.org/0000-0001-7684-0610>

Courtney A. Puckree-Padua is currently employed as a Doctor of Marine Biology at the Cape Peninsula University of Technology, South Africa. She was awarded a PhD in Algal Taxonomy by the University of the Western Cape, where her postgraduate research was conducted. Courtney used an integrated taxonomic approach to resolve the biodiversity of species previously assigned to the genus *Spongites* in South Africa. Her more recent research includes resolving the phylogenies within the Corallinales from Chile and Antarctica.



Paul W. Gabrielson

Biology Department and Herbarium, University of North Carolina at Chapel Hill, Coker Hall CB 3280, Chapel Hill, NC, 27599-3280, USA
<https://orcid.org/0000-0001-9416-1187>

Paul W. Gabrielson, a Herbarium Research Associate and Adjunct Professor of Biology at the University of North Carolina, Chapel Hill, does research on algal systematics. His two post-docs were with the esteemed phycologists Dr. Gerald T. Kraft and the late Dr. Robert F. Scagel. Paul began to re-tool from morpho-anatomy to DNA sequencing while teaching at a small, liberal arts college for nine years, before returning to North Carolina. Paul collaborates with phycologists worldwide sequencing field-collected and type specimens of seaweeds from the 18th, 19th, and early 20th centuries, especially coralline red algae.



Gavin W. Maneveldt

Department of Biodiversity and Conservation Biology, University of the Western Cape, P. Bag X17, Bellville 7535, South Africa
gmaneveldt@uwc.ac.za
<https://orcid.org/0000-0002-5656-5348>

Gavin W. Maneveldt is a Professor of Marine Biology in a small department at the University of the Western Cape, South Africa. He was initially interested in pursuing research into marine herbivore-algal interactions, but the lack of suitable names for most of the coralline algae he encountered, quickly changed that focus. Since obtaining his PhD, Gavin's interest shifted almost entirely to the taxonomy and systematics of the non-geniculate coralline red algae. Gavin collaborates extensively with phycologists of similar interest worldwide, lending his unique expertise in histology and morpho-anatomy to the understanding of the diversity of the non-geniculate coralline red algae.